



SALVADOR LOU VEGA

**Modelo Matemático para o estudo do efeito Allee sobre a
Dispersão de Plantas por Agentes e em meios
Heterogêneos**

CAMPINAS
2013



UNICAMP

Universidade Estadual de Campinas

Instituto de Matemática, Estatística
e Computação Científica

Salvador Lou Vega

Modelo Matemático para o estudo do efeito Allee sobre a
Dispersão de Plantas por Agentes e em meios
Heterogêneos

Orientador: Prof. Dr. Wilson Castro Ferreira Junior

Tese de doutorado apresentada do Instituto de
Matemática, Estatística e Computação Científica da Unicamp para
obtenção do título de Doutor em matemática aplicada.

ESTE EXEMPLAR CORRESPONDE À VERSÃO FINAL DA TESE
DEFENDIDA PELO ALUNO SALVADOR LOU VEGA,
E ORIENTADA PELO PROF. DR. WILSON CASTRO FERREIRA JUNIOR.

Assinatura do Orientador

Campinas
2013

Ficha catalográfica
Universidade Estadual de Campinas
Biblioteca do Instituto de Matemática, Estatística e Computação Científica
Ana Regina Machado - CRB 8/5467

L92m Lou Vega, Salvador, 1972-
Modelo matemático para o estudo do efeito Allee sobre a dispersão de plantas por agentes e em meios heterogêneos / Salvador Lou Vega. – Campinas, SP : [s.n.], 2013.

Orientador: Wilson Castro Ferreira Junior.
Tese (doutorado) – Universidade Estadual de Campinas, Instituto de Matemática, Estatística e Computação Científica.

1. Efeito Allee. 2. Núcleo de dispersão. 3. Plantas - Dispersão. I. Ferreira Junior, Wilson Castro, 1948-. II. Universidade Estadual de Campinas. Instituto de Matemática, Estatística e Computação Científica. III. Título.

Informações para Biblioteca Digital

Título em inglês: Mathematical model for the study of the Allee effect on the dispersal of plants by agents and in heterogeneous environments

Palavras-chave em inglês:

Allee effect

Dispersal kernels

Plants - Dispersal

Área de concentração: Matemática Aplicada

Titulação: Doutor em Matemática Aplicada

Banca examinadora:

Wilson Castro Ferreira Junior [Orientador]

Luiz Alberto Díaz Rodrigues

Norberto Anibal Maidana

Rodney Carlos Bassanezi

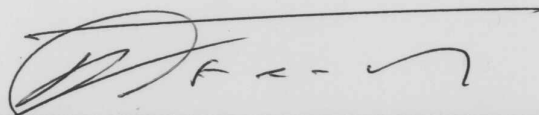
Laércio Luis Vendite

Data de defesa: 05-04-2013

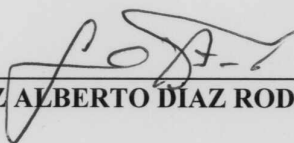
Programa de Pós-Graduação: Matemática Aplicada

Tese de Doutorado defendida em 05 de abril de 2013 e aprovada

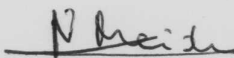
Pela Banca Examinadora composta pelos Profs. Drs.



Prof(a). Dr(a). WILSON CASTRO FERREIRA JUNIOR



Prof(a). Dr(a). LUIZ ALBERTO DÍAZ RODRIGUES



Prof(a). Dr(a). NORBERTO ANIBAL MAIDANA



Prof(a). Dr(a). RODNEY CARLOS BASSANEZI



Prof(a). Dr(a). LAÉRCIO LUIS VENDITE

Aos meus Pais e irmãos...

Agradecimentos

Ao meu orientador, Prof. Wilson Castro Ferreira Jr., pela paciência, dedicação, profissionalismo e principalmente, por todo o conhecimento e crescimento transmitidos durante o este período de estudos de pós-graduação.

Aos professores Dr. Luiz Alberto Diaz, Dr. Rodney Bassanezi, Dr. Norberto Maidana e Dr. Laércio Vendite pelas sugestões e grandes contribuições para o aprimoramento deste trabalho. Suas recomendações foram de grande valor, obrigado.

Aos secretários da SPG, Tânia, Livia e Ednaldo, pelo carinho, amizade, disposição e prestatividade durante todo o período de meus estudos de pós-graduação na UNICAMP.

À CAPES e ao Programa de Estágio Docente -PED- da UNICAMP pelo apoio financeiro.

À Patrícia Borges dos Santos, Dafne e Diego por serem minha família aqui no Brasil.

Aos meus amigos e colegas do IMECC.

À minha família, que sempre estiveram e estão ao meu lado em qualquer situação. Vocês me fortalecem, muito obrigado.

E, sobre tudo e todos, agradeço a Deus.

Resumo

Apresentamos um modelo integro-recursivo para a dispersão de uma planta que acopla uma dinâmica de reprodução com efeito Allee e uma dinâmica de dispersão em um meio heterogêneo. Propomos um modelo de difusão e sedimentação para derivar núcleos de dispersão teóricos, que representem o padrão de dispersão de sementes gerado por pássaros frugívoros em um meio heterogêneo. O núcleo gerado através do modelo é capaz de reproduzir o padrão espacial de agregação de sementes gerado pelos pássaros frugívoros sob condições naturais. Enquanto à dinâmica de reprodução, consideramos um efeito Allee devido à limitação de pólen, que reduz a produção de sementes. Introduzimos o efeito Allee através de uma função de probabilidade que depende da densidade local de plantas. Analisa-se o comportamento da expansão da planta, e estima-se a velocidade média de expansão. O modelo mostra uma invasão através de pulsos, que atribuímos ao efeito Allee e ao comportamento de dispersão da planta .

Palavras-chave: Efeito Allee, núcleos de dispersão, plantas - dispersão.

Abstract

We present an integro-difference model for a plant dispersal, which couples a reproductive dynamic with Allee effect and a dispersal dynamic in an heterogeneous environment. We propose a diffusion and settling model to derive theoretical dispersal kernels, that represent the seed dispersal pattern generated by frugivores birds in a heterogenous environment. The dispersal kernel derived through the model is able to reproduce the aggregate seed dispersal pattern generated by the frugivores birds under field conditions. As for the reproductive dynamic, we consider an Allee effect due to pollen limitation, which reduces seed production. We introduce the Allee effect through a probability function, which depends on the local plant density. The plant expansion behavior is analyzed, and the average expansion speed is estimated. The model shows a pulsed invasion, which we attribute to the Allee effect and the plant dispersal behavior.

Keywords: Allee effect, dispersal kernel, plant dispersal.

Conteúdo

Resumo	viii
Abstract	ix
Introdução	1
1 Núcleos de Dispersão Teóricos para plantas de frutos carnosos dispersadas por pássaros	3
1.1 Introduction	3
1.2 The Model	5
1.3 Results	8
1.3.1 Non-dimensional Seed Dispersal Model and the Dispersal Kernel Equation.	8
1.3.2 Numerical Results	10
1.3.3 Multiple-Scale and Homogenization technique to the Dispersal Kernel	15
1.4 Discussion	19
1.5 Conclusions	21
1.6 Appendix	22
1.6.1 Appendix A: Approximate solution to the 1D Dispersal Kernel Equation, using multiple scales and homogenization technique.	22
1.6.2 Appendix B: Approximate solution to the Dispersal Kernel in 2 dimensions, using multiple scales and homogenization techniques.	26
2 Invasão Biológica de uma planta de fruto carnosos dispersada por pássaros e sujeita a efeito Allee	31
2.1 Introduction	31
2.2 The model	34
2.2.1 Local Dynamics: growth, reproduction and seed output	34
2.2.2 Spatial Dynamics: Seed dispersal	37
2.2.3 Dispersal Kernel	37
2.3 Results	38
2.3.1 Local Dynamics: Growth model	38
2.3.2 Spatial Dynamics: Dispersal Process	40
2.3.3 Discussion	48

2.4 Conclusions	50
Conclusões Gerais	52
Referência Bibliográfica	56

Introdução

Uma abordagem para o entendimento do processo de invasão de organismos é possível através de modelos matemáticos. Os modelos matemáticos que descrevem a expansão de uma população basicamente acoplam uma dinâmica de reprodução e uma de dispersão. Os primeiros modelos matemáticos a modelar a expansão de organismos foram os de Skellam (1951) e Fisher (1937). Se bem que estes modelos baseados em equações de reação e difusão predizem razoavelmente a expansão de algumas invasões, existem outros casos em que a predição da expansão dada por estes modelos não é adequada (Hastings et al., 2005). Os modelos de Skellam e Fisher serviram como plataforma para o desenvolvimento de outros modelos mais complexos e realistas (Hastings et al., 2005; Taylor and Hastings, 2005). Existem modelos gerais sobre expansão e invasão, mas também tem-se desenvolvido modelos específicos para espécies invasoras em particular (Johnson et al., 2006; Takasu et al., 2000).

Novos modelos de invasão incorporam mais detalhes sobre o crescimento populacional e os mecanismos de dispersão. Estes ingredientes tornam mais realistas os modelos, fornecendo informação mais detalhada sobre o processo de invasão e como controlar as invasões. A recente utilização de equações íntegro-recursivas para a modelagem de expansão, abriu uma grande possibilidade de incorporar diferentes padrões de dispersão (Kot et al., 1996). As equações íntegro-recursivas incorporam diferentes padrões de dispersão através dos núcleos de dispersão. Os núcleos de dispersão são distribuições de densidade de probabilidade, que resumem a probabilidade de um organismo localizado em um ponto x , se dispersar a uma localidade y .

A derivação dos núcleos de dispersão é de muita importância, pois influenciam a dinâmica de expansão. Os núcleos de dispersão são obtidos principalmente de forma fenomenológica, ajustando curvas de distribuições a dados experimentais de dispersão. No entanto, também há alguns exemplos e tentativas para desenvolver núcleos de dispersão teóricos. No caso de plantas, as sementes são a fase da população que se dispersa. Modelos teóricos para descrever a dispersão de sementes têm sido desenvolvidos satisfatoriamente para o caso daquelas dispersas pelo vento. Para o caso de sementes zoócoras, aquelas dispersas por animais, o seu desenvolvimento é menor, principalmente pela dificuldade de modelar o movimento dos animais. Em teoria, a derivação de núcleos de dispersão de sementes por animais, precisam da seguinte informação: a) comportamento e taxa de movimentação dos animais, e b) taxa de passagem das sementes através do tracto digestivo.

No capítulo primeiro desta tese, trataremos da derivação terica de núcleos de dispersão de sementes por animais frugívoros, isto é por animais que consomem os frutos carnosos de plantas e

em consequência dispersam as sementes ingeridas. A derivação baseia-se nos trabalhos de Neubert et al. (1995) e Powell and Zimmermann (2004). Estes autores propõem modelos de difusão e sedimentação para a dispersão de sementes por animais. O modelo proposto nesta tese, introduz de forma simples a movimentação dos animais num meio heterogêneo e incorpora uma taxa de passagem de sementes. Através de técnicas de múltiplas escalas e homogeneização consegue-se dar uma expressão analítica para a aproximação do núcleo de dispersão. Os núcleos de dispersão gerados através do modelo proposto, geram uma distribuição espacial heterogênea das sementes, caracterizando-se por apresentar pontos de agregação de sementes. Este padrão espacial é observado em plantas dispersas por aves frugívoras.

Por outro lado, a incorporação do efeito Allee na dinâmica de reprodução nos modelos de invasão tem-se tornado importante recentemente (Taylor and Hastings, 2005). O efeito Allee pode alterar a dinâmica de invasão de várias formas como reduzindo a velocidade de expansão (Kot et al., 1996), ou introduzindo limiares para o êxito de uma invasão (Lewis and Kareiva, 1993; Kot et al., 1996). Também é considerado responsável dos períodos de latência ("*lag phase*") nas invasões (Parker, 2004), e de formação de padrões (Petrovskii et al., 2002; Mistro et al., 2012). Estes dois fenômenos fazem com que o comportamento da expansão da frente da invasão não seja de forma suave e contínua como predizem de forma geral os modelos IRE ou RDE. O efeito Allee pode surgir sempre que a população apresente densidades muito baixas. Estas situações podem ocorrer na fase de colonização, ou na frente de uma invasão. Em um estudo realizado por Davis et al. (2004), encontrou-se que a população invasora da espécie *Spartina alterniflora* estava sujeita ao efeito Allee devido a falta de pólen na frente da invasão.

O segundo capítulo da tese, baseia-se na descoberta de (Davis et al., 2004) e analisa-se o comportamento da expansão da população de plantas, visando observar os efeitos de retardamento ou formação de padrões atribuídos ao efeito Allee. Modela-se a expansão de uma planta sujeita ao efeito Allee devido à falta de pólen, e considera-se um comportamento de dispersão de acordo ao núcleo de dispersão gerado no capítulo um.

Capítulo 1

Núcleos de Dispersão Teóricos para plantas de frutos carnosos dispersadas por pássaros

Theoretical Dispersal Kernels for fleshy fruited plant species dispersed by birds

Abstract. We attempt to derive a theoretical seed dispersal kernel for a plant, whose seeds are dispersed by frugivores animals, principally birds. We use a diffusion and settling model framework. We assume that seeds follow the frugivores animals, and model the animals' movement as the continuous approximation of an unbiased brownian motion in heterogeneous environment. We assume a periodic environment, where the frugivores diffuse at different rates, low diffusion rates at sites where they use to settle and high diffusion rates between these sites. We use a multiscale and homogenization technique to obtain an analytical approximation to the dispersal kernel. The technique approximated well the numerical solution of the dispersal kernel. Different dispersal kernels arise when varying the distance between the settling sites and the rates of movement of the frugivores. Smaller distances between settling sites generate a more uneven seed distribution, whether higher rates of diffusion yield dispersal kernels with fatter tails.

1.1 Introduction

Seed dispersal is a key process in plant spatial dynamics, it contributes to determine the local frequency and abundance of plants. Models of seed dispersal have been important in representing seed density distributions and investigating dispersal processes among other things. The spatial

distribution of seeds dispersed, the "seed shadow", is represented by curves (one dimension) or surfaces (two dimension) that summarizes the distribution of distances traveled by seeds. Dispersal curves have been coined as distance distributions, dispersal kernels or probability density functions (Nathan and Muller-Landau, 2000). In mathematical terms, a dispersal kernel, $K(x-\xi)$, expresses the probability of a seed dispersing a distance, $|x-\xi|$, from a parent located at ξ to a location x . The number of seeds produced per plant multiplied by its dispersal kernel is referred as the "seed shadow". The combination of seed shadows from different individuals of a plant species is known as the seed rain. The entire distribution of dispersal distances is critical to range expansion rates, recruitment patterns, genetic structure, etc. (Levin et al., 2003), hence, an accurate representation of the seed shadow is of fundamental importance.

Dispersal kernels can be estimated by fitting a curve to field data on seed densities as a function of distance from a source (phenomenological models) (Nathan and Muller-Landau, 2000). Dispersal curves can in principle form any kind of distribution. However, three functional forms have been commonly fitted to dispersal data: the Gaussian, the negative exponential and the inverse power law (Levin et al., 2003; Nathan and Muller-Landau, 2000).

Dispersal kernels can be derived theoretically through mechanistic models. These models, use precise knowledge of the characteristics of the seed dispersal process, to develop a theoretical (mathematical) model, through which, a seed dispersal curve is derived.

To understand seed dispersal, requires the development of mechanistic models that can explain the observed patterns. These models can predict the exact seed distribution from characteristics of the dispersal processes. Mechanistic models for wind dispersed seeds have a long history (Okubo and Levin, 1989). They use information on wind conditions and plant attributes to predict the spatial pattern of the seeds dispersed (Nathan and Muller-Landau, 2000). In general, mechanistic models for wind dispersed seeds predict a peak of seeds at the source or near it, and then a continuous decline in seed density with distance from the peak (Okubo and Levin, 1989). Models of seed dispersal by animals are less developed, in part, because such models require quantification of behavioral information (Levin et al., 2003). In theory, knowledge of the animal behavior and plant attributes can be combined to predict seed dispersal by animals (Nathan and Muller-Landau, 2000, Levin et al., 2003). Under field conditions it is observed that animal dispersed seed density, does not decline in a continuous and simple way with distance from source (Kollmann, 2000). Animal behavior is one of the main factors in determining the spatial pattern of animal dispersed seeds (Russo et al. 2006, Westcott et al. 2005). Habitat heterogeneity plays a significant role in determining seed distribution patterns, since animal behavior is affected by local vegetation structure (Kollmann, 2000). Bird-mediated seed rain, for example, is generally sparse in open areas, and heavily concentrated under perches such as isolated trees, or under clusters of bushes or trees, forest gaps, etc. (Kollmann 2000). Some fruit bats tend to concentrate seeds under feeding roosts. Perches and feeding roosts are commonly described as "recruitment foci" (Kollmann, 2000). The vegetation structure and the animal feeding behavior can generate a spatially aggregated distribution of seeds. Hence, traditional dispersal curves may underestimate the clumping or aggregated distribution of animal dispersed seeds. The aggregate distribution observed under field conditions should be reflected in a multi-modality seed dispersal curve (Westcott et al., 2005,

Russo et al., 2006). Models that attempt to describe the seed dispersal by animals are based on seed passage times and mean displacement rates of animals (Murray, 1988, Westcott et al., 2005), or on stochastic, spatially explicit models that incorporate animal movements (Russo et al., 2006). These models describe, through frequency distributions of dispersal distance, the aggregated spatial pattern of animal dispersed seeds (Westcott et al., 2005, Murray, 1988, Russo et al., 2006), suggesting the use of a multi-modality function for the representation of the dispersal curve (Russo et al., 2006). However, by fitting a curve or several curves to the frequency distributions, the parameters of the resulting dispersal kernel, do not represent biological attributes of the dispersal process. Although, these models use biological information to construct a dispersal kernel, they lack a theoretical framework, that enables the analysis of the processes behind the patterns.

Few theoretical models have been developed to derive dispersal kernels for animal dispersed seeds (Neubert et al., 1995, Powell and Zimmermann, 2004).

Neubert et al. (1995) modeled dispersal as the diffusion of propagules in a homogeneous environment, that settle at ground at a certain rate. They modeled seed dispersal through brownian motion in homogeneous environment. The model is simple and the dispersal kernel derived by the model is expressed by an analytical function.

Powell and Zimmermann (2004) used same approach for dispersal of seeds by animals caching seeds. They used Fickian diffusion in a heterogeneous environment to model animal dispersal, and assumed a spatial seed deposition probability (where the animals cached seeds). The model is able to represent the clumping distribution of seeds, but its solution is obtained by numerical methods. A multi-scale analysis and a homogenization technique was applied to the model, in order to get an analytical approximation of the dispersal kernel. Although, the approximation fail to reproduce the aggregate distribution of seeds, it gave good estimates on expansion rates, which was the main goal of their work.

In this paper, we propose a model for animal seed dispersal in a heterogeneous environment, following Neubert et al. (1995) and Powell and Zimmermann (2004) approach. We aim to derive a dispersal kernel which reflects the aggregate distribution of seeds. Through a multiple scale analysis and homogenization technique we attempt to obtain an analytical approximation to the kernel, which retains the clumping distribution of seeds dispersed.

1.2 The Model

Neubert et al. (1995) derived a theoretical dispersal kernel, modeling dispersal as the diffusion of propagules that settle with a certain rate. If diffusion is taking as an unbiased random walk in a homogeneous environment, and the propagules are released from a point ξ , the probability density of propagules at any time t , in the air $P(x, t)$ and at the ground $S(x, t)$ satisfies:

$$\begin{cases} \frac{\partial P}{\partial t} = D \frac{\partial^2 P}{\partial x^2} - \lambda(t)P, & \frac{\partial S}{\partial t} = \lambda(t)P \\ P(x, 0) = \delta(x - \xi). & S(x, 0) = 0. \end{cases}$$

where D is the diffusion coefficient and $\lambda(t)$ is the settling rate. The dispersal kernel $K(x - \xi)$ is obtained as the distribution of seeds on the ground $S(x, t)$ when time goes to infinity:

$$K(x - \xi) = \lim_{t \rightarrow \infty} S(x, t).$$

For a constant settle rate $\lambda(t) = \lambda$, Neubert et al. (1995) obtained the Laplace or double exponential kernel,

$$K(x - \xi) = \frac{1}{2} \sqrt{\frac{\lambda}{D}} \exp\left(-\sqrt{\frac{\lambda}{D}}|x|\right).$$

Powell and Zimmermann (2004) used Neubert et al. (1995) approach for the dispersal of seeds by animal cashers. They modeled seed dispersal as the diffusion of animal dispersers that caches seeds in certain locations. Since animal dispersers do not deposit seeds randomly or with equal probability, Powell and Zimmermann (2004) considered that the diffusion of dispersers (D) and ‘settling’ or caching (λ) of seeds should be functions of space. Dispersers move seeds rapidly (high D) between cache areas, where seeds are unlikely to be deposited (low λ). Conversely, seed dispersers spend more time in a small area (low D) where the seeds are dropped and stored in small cached areas (high λ). Thus, the diffusion and settling functions are anti-correlated. Using Fickian diffusion, and a function representing the probability of caching seeds in space ($\lambda(x)$), the model for seed dispersal by animal cashers from a point of release, becomes Powell and Zimmermann (2004)

$$\begin{cases} \frac{\partial P}{\partial t} = \frac{\partial}{\partial x} \left(D(x) \frac{\partial P}{\partial x} \right) - \lambda(x)P, & \frac{\partial S}{\partial t} = \lambda(x)P \\ P(x, 0) = \delta(x - \xi). & S(x, 0) = 0. \end{cases}$$

For the diffusion and settling, Powell and Zimmermann (2004) used periodic piecewise constant functions. Using a multi-scale analysis and homogenization techniques they obtained the homogenized kernel of the model:

$$K_{hom}(x - \xi) = \frac{1}{2} \sqrt{\frac{\hat{\lambda}}{\hat{D}}} \exp\left(-\sqrt{\frac{\hat{\lambda}}{\hat{D}}}|x|\right).$$

where $\hat{D}, \hat{\lambda}$ are the homogenized constants of the diffusion and settling parameters. These homogenized parameters are spatially independent and their values are the harmonic mean of the diffusion and settling functions.

Following Neubert et al. (1995) and Powell and Zimmermann (2004), we want to derive, as simple as possible, a theoretical kernel for an animal dispersed plant, which is able to represent the aggregate spatial pattern observed under field conditions. This type of seed shadow is commonly seen in fleshy-fruited plant species, which rely on birds or bats for its dispersal.

Animal seed dispersal is frequently modeled combining information on animal movement behavior and seed gut passage time. Considering that seeds follow animal movements, we modeled seed dispersal as the diffusion of animal dispersers that defecate seeds ('settling of seeds') in the air at a certain rate. We take diffusion as the continuous approximation of discrete uncorrelated random walk performed by animal dispersers. This is a simple form to model animals' movement without directional persistence (Turchin, 1998). This type of diffusion is referred as "*ecological diffusion*" (Turchin, 1998) or "*biodiffusion*" (Okubo and Levin, 2001). A clear and simple derivation of the ecological diffusion may be found in Turchin (1998). Animals' movement in general are affected by the environment (vegetation structure for example) and time. Here we assume that animal dispersers' movement depends only on space. For the settling rate, we take the rate of seed passage, and for simplicity, let us assume it, to be constant ($\lambda(t) = \lambda$). Our model for seed dispersal by animals is

$$\begin{cases} \frac{\partial P}{\partial t} = \frac{\partial^2}{\partial x^2}(D(x)P) - \lambda P, & \frac{\partial S}{\partial t} = \lambda P, \\ P(x, 0) = \delta(x - \xi). & S(x, 0) = 0. \end{cases} \quad (1.1)$$

where $P(x, t)$ is the density of seeds in movement at any spatial location x and time t , $S(x, t)$ is the probability density distribution of seeds at ground at any time t . Diffusion, $D(x)$, represents the motility of the animal dispersers, hence, the motility of seeds. The desired dispersal kernel $K(x)$ is obtained as the limit of time to infinity of the distribution of seeds at ground: $K(x) = \lim_{t \rightarrow \infty} S(x, t)$.

The model can easily be extended spatially to two dimensions $\mathbf{x} = (x_1, x_2)$:

$$\begin{cases} \frac{\partial P}{\partial t} = \nabla^2(D(\mathbf{x})P) - \lambda(t)P, & \frac{\partial S}{\partial t} = \lambda(t)P, \\ P(\mathbf{x}, 0) = \delta(\mathbf{x} - \xi). & S(\mathbf{x}, 0) = 0. \end{cases} \quad (1.2)$$

Animals in general do not move constantly through time, they move and settle, then move again and settle. Distance traveled, velocity and site of settling depends on the animals' behavior and on the environment. Animal dispersers such as birds or bats, tend to fly to their feeding plants, spend some time picking fruits and then leave the plant, to settle in a perch, feeding roost, latrines, different habitats like forest gaps or vegetation of different successional stages, etc. Thus, we have a high motility (high D) of seeds when the animal disperser is in move (for example flying), and

a low motility (low D) of seeds as the animal settles. Therefore, the diffusion function, $D(x)$, should vary in space between high and low D , furthermore, it may reach its minimum, D_{min} , at the settling sites and a maximum, D_{max} , between settling sites.

Settling sites may be distributed in a heterogeneous and random way in space. To introduce these heterogeneity in the model, we can hypothetically consider a landscape where the vegetation features the animal uses to settle vary in a periodic way. A simple way to represent diffusion in such environment is through positive trigonometric and periodic function.

1.3 Results

1.3.1 Non-dimensional Seed Dispersal Model and the Dispersal Kernel Equation.

Let A be the difference between the maximum and minimum diffusion of the animal disperser ($A = D_{max} - D_{min}$). The parameter A has dimension of diffusion [distance²/time]. The rate of seed passage, λ , has dimension [1/time]. In order to obtain the non-dimensional models of (1.1) and (1.2), we scale the spatial and time variables to the parameters A and λ .

1D Dispersal Model

Introducing the non-dimensional space ξ and time τ variables:

$$\xi = \sqrt{\frac{\lambda}{A}}x, \quad \tau = \lambda t, \quad (1.3)$$

in equation (1.1), yields

$$\begin{cases} \frac{\partial P}{\partial \tau} = \frac{\partial^2}{\partial \xi^2} \left(\frac{1}{A} D(\xi) P \right) - P, & \frac{\partial S}{\partial \tau} = P, \\ P(\xi, 0) = \delta(\xi - \xi_0). & S(\xi, 0) = 0. \end{cases} \quad (1.4)$$

For the diffusion, we may choose the trigonometric periodic function

$$D(x) = A \left[\frac{1}{2} \sin \left(ax + \frac{\pi}{2} \right) + \frac{1}{2} \right] + B; \quad (1.5)$$

where a is the frequency of settling sites, A and B are positive constants. Note that $D_{max} = A + B$, and $D_{min} = B$. Introducing the non-dimensional parameters: $\gamma = B/A$ and $\omega = a\sqrt{A/\lambda}$, the non-dimensional diffusion function is given by

$$\mathcal{D}(\omega\xi) = \frac{1}{A}D(\xi) = \frac{1}{2}\sin\left(\omega\xi + \frac{\pi}{2}\right) + \frac{1}{2} + \gamma, \quad (1.6)$$

where we have expressed the frequency, ω , explicitly in the diffusion's argument. Integrating equations in (1.4) in relation to the variable time τ , from $\tau = 0$ to infinity we have that the dispersal kernel $K(\xi) = \lim_{\tau \rightarrow \infty} S(\xi, \tau)$ satisfies the equation

$$\frac{\partial^2}{\partial \xi^2} (\mathcal{D}(\xi)K) - K = -\delta(\xi - \xi_0), \quad (1.7)$$

where $K(\xi) = \int_0^\infty P(\xi, \tau)d\tau$. For a standard nomenclature we may replace the variables (ξ, \mathcal{D}) for (x, D) , thus the Dispersal Kernel equation may be written as

$$\frac{\partial^2}{\partial x^2} (D(x)K) - K = -\delta(x - \xi_0). \quad (1.8)$$

2D Dispersal Model

For the two dimensional model (1.2), we introduce the space $\xi = (\xi_1, \xi_2)$ and time τ variables:

$$\xi = \sqrt{\frac{\lambda}{A}}\mathbf{x}, \quad \xi_1 = \sqrt{\frac{\lambda}{A}}x_1, \quad \xi_2 = \sqrt{\frac{\lambda}{A}}x_2, \quad \tau = \lambda t. \quad (1.9)$$

The non-dimensional model (1.2) becomes

$$\begin{cases} \frac{\partial P}{\partial \tau} = \nabla^2(\frac{1}{A}D(\xi)P) - P, & \frac{\partial S}{\partial \tau} = P, \\ P(\xi, 0) = \delta(\xi - \xi_0). & S(\xi, 0) = 0. \end{cases} \quad (1.10)$$

For the diffusion in two dimensions, we may choose the following trigonometric periodic functions:

$$D(\mathbf{x}) = A \left[\frac{1}{2} \sin \left(a\sqrt{x_1^2 + x_2^2} + \frac{\pi}{2} \right) + \frac{1}{2} \right] + B; \quad (1.11)$$

or

$$D(\mathbf{x}) = A \left[\frac{1}{2} \sin \left(ax_1 + \frac{\pi}{2} \right) \sin \left(bx_2 + \frac{\pi}{2} \right) + \frac{1}{2} \right] + B; \quad (1.12)$$

where a and b are the frequency of settling sites in the x_1 and x_2 directions respectively, $D_{max} = A + B$, and $D_{min} = B$. Introducing the non-dimensional parameters: $\gamma = B/A$, $\omega_1 = a\sqrt{A/\lambda}$, and $\omega_2 = b\sqrt{A/\lambda}$ the non-dimensional diffusion function are given by

$$\mathcal{D}(\xi) = \frac{1}{2} \sin \left(\omega \sqrt{\xi_1^2 + \xi_2^2} + \frac{\pi}{2} \right) + \frac{1}{2} + \gamma, \quad (1.13)$$

$$\mathcal{D}(\xi) = \frac{1}{2} \sin \left(\omega_1 \xi_1 + \frac{\pi}{2} \right) \sin \left(\omega_2 \xi_2 + \frac{\pi}{2} \right) + \frac{1}{2} + \gamma. \quad (1.14)$$

Integrating equation (1.2) in the variable time τ , from $\tau = 0$ to infinity, we have that the dispersal kernel in two dimensions $K(\xi) = \lim_{\tau \rightarrow \infty} S(\xi, \tau)$ satisfies the equation

$$\nabla^2(\mathcal{D}(\xi)K) - K = -\delta(\xi - \xi_0), \quad (1.15)$$

where $K(\xi) = \int_0^\infty P(\xi, \tau) d\tau$. Here too, we may replace (ξ, \mathcal{D}) for (\mathbf{x}, D) , thus the two dimensional dispersal kernel equation may be written as

$$\nabla^2(D(\mathbf{x})K) - K = -\delta(\mathbf{x} - \xi_0) \quad (1.16)$$

1.3.2 Numerical Results

The non-dimensional models (1.8) and (1.13), depend on the 3 parameters: ω, γ and ξ_0 . The parameter ξ_0 represents the location of the source plant whose seeds are dispersed.

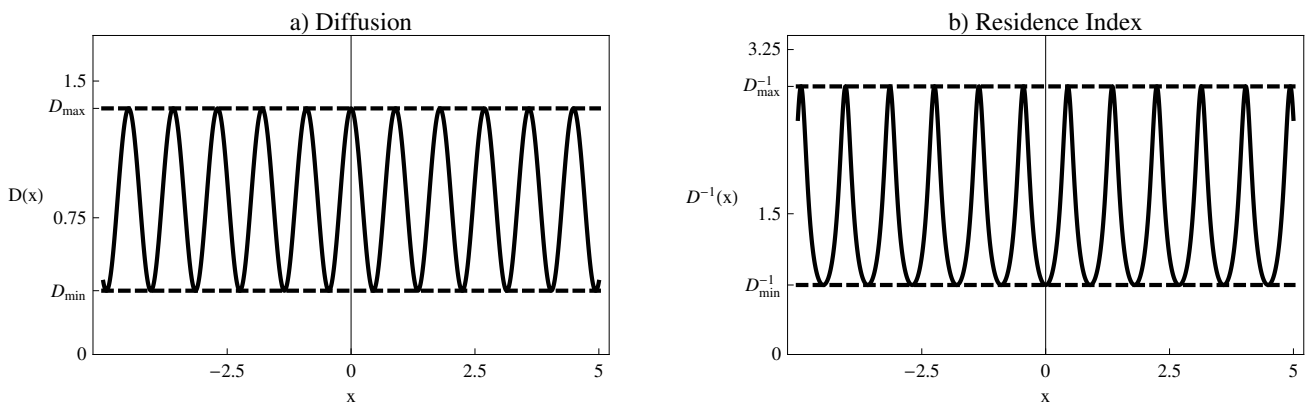


Figure 1.1: a) Diffusion ($D(x)$). Maximum and minimum diffusion are shown, D_{max} and D_{min} respectively, (dashed lines); b) Residence Index D^{-1} . Maximum and minimum residence time are shown, $D_{max}^{-1} = \gamma^{-1}$ and D_{min}^{-1} respectively (dashed lines). Parameters used : $\gamma = 0, 35$; Diffusion function: $D(\omega x) = \frac{1}{2} \sin(\omega x + \frac{\pi}{2}) + \frac{1}{2} + \gamma$.

The frequency of the settling sites is given by the parameter ω . The inverse of the frequency [$1/\omega$] is a measure of the distance between the sites the animal disperser uses to settle. The parameter

γ represents the minimum diffusion (D_{min}) of the animal disperser or the seed in movement. The inverse of the diffusion D^{-1} , is referred as the residence index. It gives a measure of the time spent by an animal at a given location (Turchin (1998), Okubo and Levin (2001), hence, γ^{-1} gives an estimate of the residence time of the the animal disperser at the settling sites. Figure 1.1. shows the graphs of diffusion and residence index for the diffusion function chosen for the simulations.

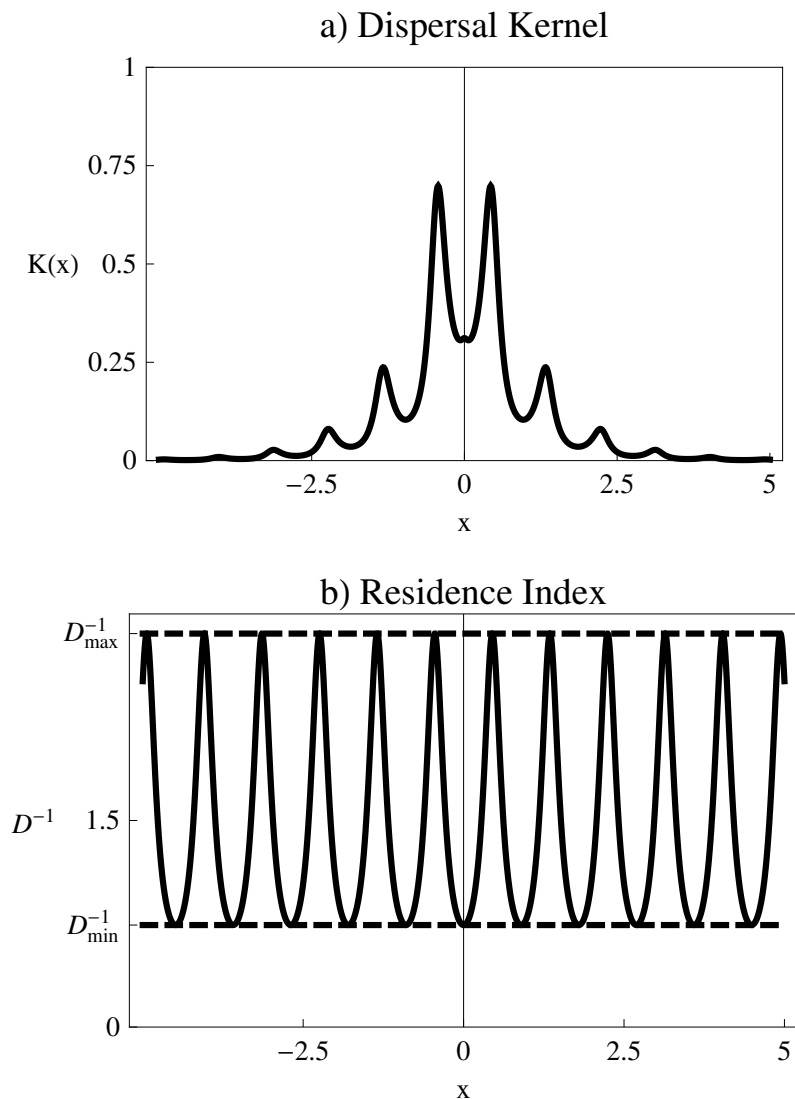


Figure 1.2: a) Dispersal Kernel. b) Residence Index $D^{-1}(x)$. Parameters used : $\omega = 7; \gamma = 0,35$; Diffusion function: $D(\omega x) = \frac{1}{2} \sin(\omega x + \frac{\pi}{2}) + \frac{1}{2} + \gamma$.

First, we explore the effects of the parameters ω and γ on the one dimensional model, considering the source plant located at the origin ($\xi_0 = 0$). We solve the model (1.8) numerically, using finite difference methods.

Figure 1.2.a. shows the seed shadow generated by the 1D model for some fixed parameters. The seed distribution shows various peaks of different seed densities. The location of the different peaks or seed aggregations, corresponds to the settling sites in the environment. These sites are, where the animal disperser shows its minimum diffusion, or in other words has its higher residence time (Figure 1.2.b). The concentration of seeds at each peak declines with distance from the source, in an exponentially way probably.

The effect of fixing the the residence time, (γ^{-1}), of an animal disperser and varying the distance between settling sites (ω) is shown in Figure 1.3.

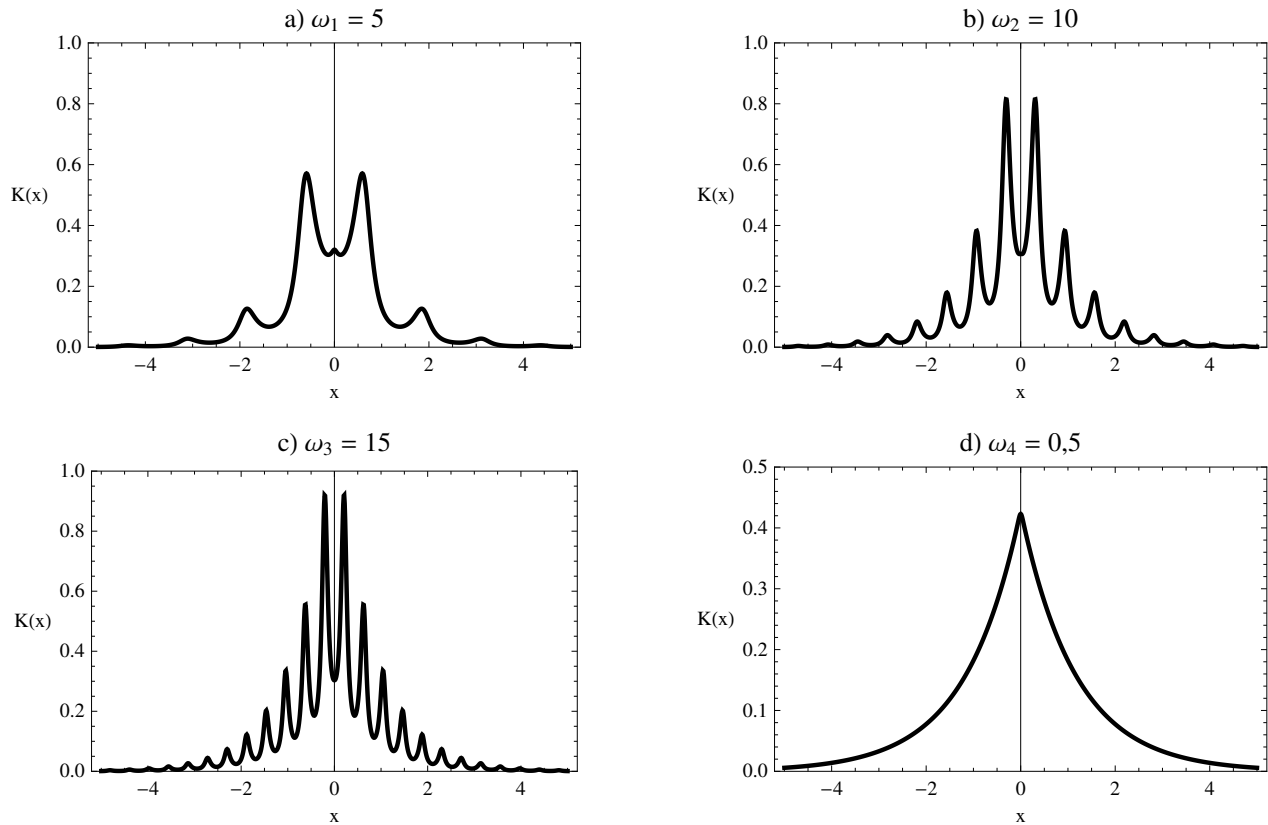


Figure 1.3: Dispersal Kernels varying the distance between settling sites ($2\pi/\omega$): a) $2\pi/\omega \approx 1, 25$; b) $2\pi/\omega \approx 0, 63$; c) $2\pi/\omega \approx 0, 42$; and d) $\omega_4 = 0, 5$. Parameters used : $\gamma = 0, 35$; Diffusion function: $D(\omega x) = \frac{1}{2} \sin(\omega x + \frac{\pi}{2}) + \frac{1}{2} + \gamma$.

Smaller distances between settling sites (large ω), generate a more concentrated aggregation (higher peaks) at the settling sites, with a narrow dispersion of seeds around them. As distance, between these sites increases (smaller ω), the concentration at each peak declines, but the seeds are more scattered around them.

For settling sites very far from each other, which means very small values of ω ($\omega < 1$), and far from the mother plant, the resulting seed shadow resembles the Laplace or double exponential distribution (Figure 1.2.d.). In this case the time that takes an animal disperser to reach a settling

site is greater than the seed passage time, so that the animal disperser has a higher probability of defecating or dropping the seeds long before it reaches a perch or feeding roost, etc.

Differences in seed density, between slow and high motility sites, are greater for higher values of ω , which generates a more heterogeneous seed distribution (Figure 1.3.c). Conversely, when ω is small, a more quantity of seeds are allowed to be deposited in between settling sites, since they are further away, creating a more even seed shadow (Figures 1.3.a and 1.3.d).

Now, the result of fixing the distance between the settling sites, and varying the residence time at the settling sites is shown in Figure 1.4.. For larger residence times, the seeds tend to travel shorter distances, making the distribution less dispersed, and with a thinner tail. On the other hand, smaller residence times, result in a wider dispersal distribution with fatter tail. This means that the seeds have a more probability to be dispersed further away and thus to increase the probability of long distance dispersal.

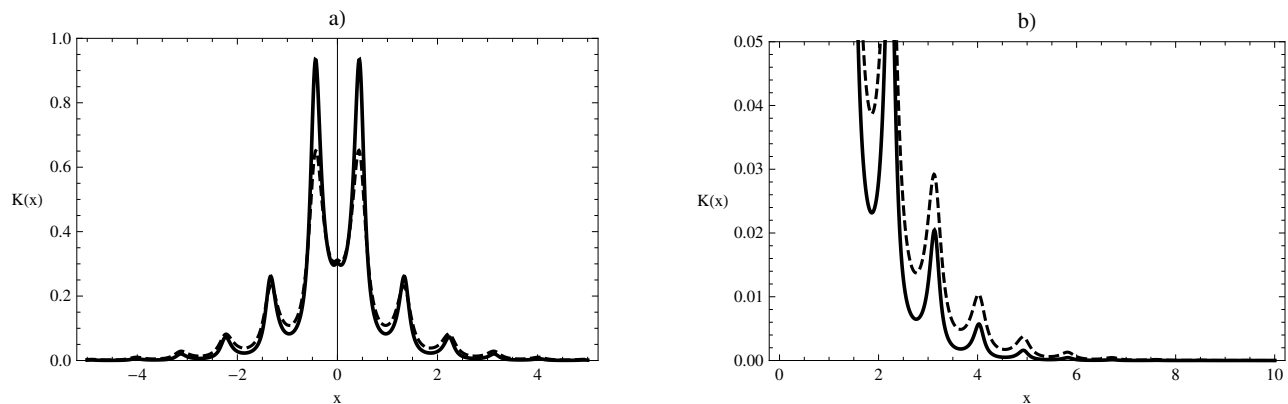


Figure 1.4: a) Dispersal Kernels varying the residence index at the settling sites (γ^{-1}): solid line $\gamma = 0, 2$; dashed line $\gamma = 0, 4$. b) Dispersal Kernel distribution tail:solid line $\gamma = 0, 2$; dashed line $\gamma = 0, 4$. Parameters used : $\omega = 7$, and $D(\omega x) = \frac{1}{2} \sin(\omega x + \frac{\pi}{2}) + \frac{1}{2} + \gamma$.

The parameter ξ_0 , determines the location of the mother plant. The location of the plant is independent of the location of the settling sites, consequently, the seed source is independent of the heterogeneity of the environment. Until now we have chosen the location of the plant at the origin ($\xi_0 = 0$). If we move the location of the mother plant, the resulting dispersal kernel may not be symmetrical. Figure 1.5 shows an anti-symmetrical distribution for a different seed source location.

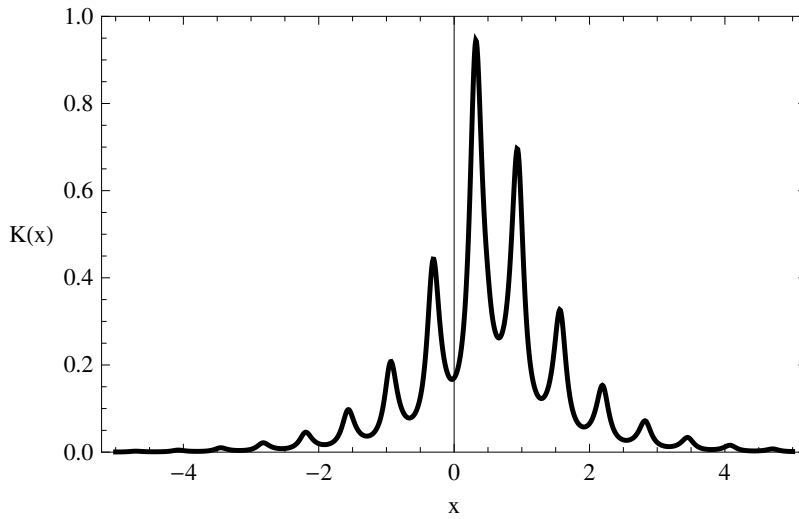


Figure 1.5: Dispersal Kernels for a release point $\xi_0 = 0,5$. Parameters used: $\omega = 10; \gamma = 0,35$. Diffusion function: $D(\omega x) = \frac{1}{2} \sin(\omega x + \frac{\pi}{2}) + \frac{1}{2} + \gamma$.

We solve numerically the two dimensional dispersal kernel equation, using difference methods. The 2D dispersal kernels have the same behavior as 1D, nonetheless, the heterogeneity of the environment has a richer representation, varying differently the frequency of the settling sites in the x and y directions. Figure 1.6. shows a 2D dispersal kernel and Figure 1.7. its contour plot.

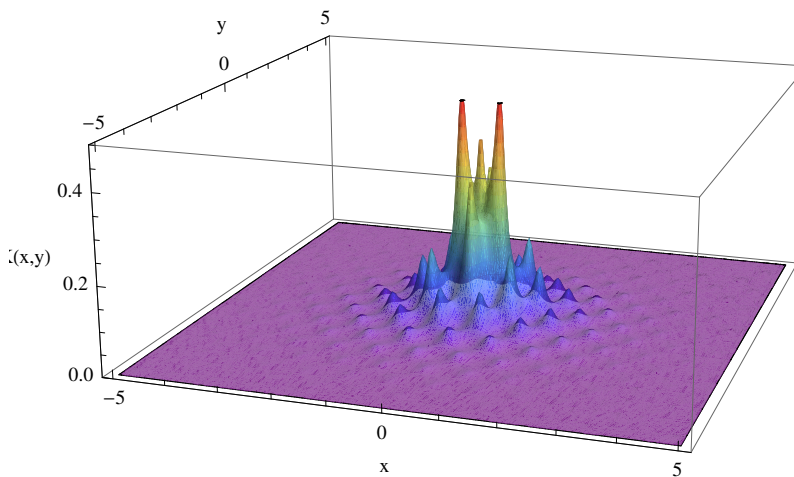


Figure 1.6: Dispersal Kernels in two dimensions. Parameters used: $\omega = (8, 5); \gamma = 0,35$. Diffusion function: $D(\omega x) = \frac{1}{2} \sin(8x + \frac{\pi}{2}) \sin(5x + \frac{\pi}{2}) + \frac{1}{2} + \gamma$.

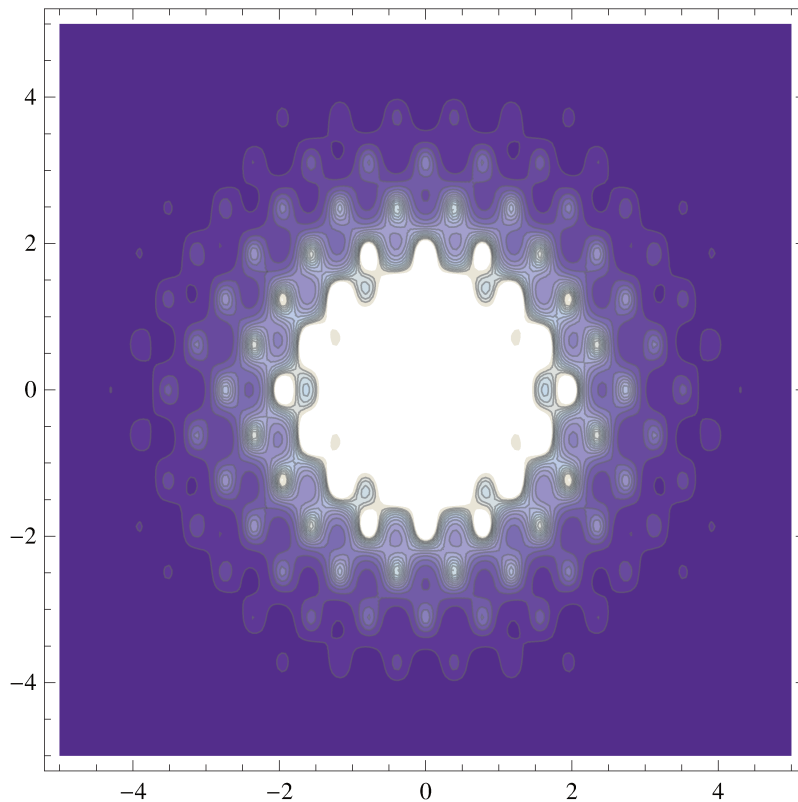


Figure 1.7: Contour Plot of the Dispersal Kernel in two dimensions. Parameters used: $\omega = (8, 5)$; $\gamma = 0, 35$. Diffusion function: $D(\omega x) = \frac{1}{2} \sin(8x + \frac{\pi}{2}) \sin(5x + \frac{\pi}{2}) + \frac{1}{2} + \gamma$.

1.3.3 Multiple-Scale and Homogenization technique to the Dispersal Kernel

In the last section we solve the Dispersal Kernel equation numerically, and showed the behavior of the solution in relation to the parameters. A dispersal kernel is useful to describe the seed distribution pattern, but its utility is wide more important in modeling plant dispersal, principally when using integro-difference or integro-differential models.

Although numerical kernels serve for the purpose of modeling plant dispersal, they fail to provide analytical estimations of expansion speeds and thresholds, which are relevant information when studying plant dispersal.

Analytical expressions are very useful and when possible always required. With an analytical expression one can visualize in a direct way the dependence on the parameters and variables.

Here we find an analytical approximation to the solution of the Dispersal Kernel equation (1.8), using multiple scales and homogenization technique.

1D Dispersal Model Approximation

In Figure 1.2 the numerical solution to the dispersal kernel equation (1.8) is shown for a particular choice of parameters (ω, γ, ξ_0) and using equation (1.6) as the diffusion function. It can be observed from the graph that there are (at least) two space scales. There is a fast scale associated with the oscillations in the solution, and there is a slower scale involved with the variation of the amplitude of the oscillations. Oscillations take place at a scale proportional to the period of the oscillations $p = 2\pi/\omega$ (ω is the frequency of the oscillations). We assume that variations at the fast scale are of order $\mathcal{O}(1/\omega)$, while the decay of the amplitude of the oscillations are of order $\mathcal{O}(1)$.

Given the disparity of the two length scales, we use a multiple scale technique to find an approximation of the solution of the dispersal kernel equation (Holmes, 1995). We begin by introducing a small parameter $\epsilon < 1$, which relates both space scales, and has a magnifying effect on the small scale. Since the small scale is of order $(\mathcal{O}(1/\omega))$ we choose $\epsilon = 1/\omega$ with $\omega > 1$. To incorporate the two space scales into the problem (1.8), we define the following space variables

$$y = \frac{x}{\epsilon}, \quad x = x. \quad (1.17)$$

These variables represent the fast and slow scales respectively. Variations of order $\mathcal{O}(1)$ in the y variable, become small variations $(\mathcal{O}(\epsilon))$ in the x variable. Introducing these variables into the dispersal kernel equation, and treating them as independent variables, the differential equation (1.8) with the diffusion function given by (1.6), takes the form (for details see Appendix A and Holmes, 1995)

$$(\partial_y^2 + 2\partial_y\partial_x + \epsilon^2\partial_x^2)(D(y)K) - \epsilon^2K = -\epsilon^2\delta(x - \xi), \quad (1.18)$$

where $\partial_y = \frac{\partial}{\partial y}$. From (1.17) we have $\omega x = x/\epsilon = y$, so that the diffusion function (1.6) with the new variables becomes

$$D(y) = \frac{1}{2} \sin\left(y + \frac{\pi}{2}\right) + \frac{1}{2} + \gamma. \quad (1.19)$$

Note that $D(y)$ is 2π -periodic, and depends only on the fast variable. Now we assume a regular asymptotic expansion for K of the form

$$K \sim K_0(x, y) + \epsilon K_1(x, y) + \epsilon^2 K_2(x, y) + \dots \quad (1.20)$$

and substitute in equation (1.18). The first term approximation to the solution of the partial differential equation (1.18) is given by (see Appendix for details)

$$K_0(x, y) = \frac{1}{D(y)} \frac{1}{2\sqrt{\langle D^{-1} \rangle}} \exp^{-|x-\xi|\sqrt{\langle D^{-1} \rangle}}, \quad (1.21)$$

where $\langle D^{-1} \rangle$ is the harmonic mean of the diffusion function (1.19) over the domain \mathbf{R}

$$\langle D^{-1} \rangle = \lim_{y \rightarrow \infty} \frac{1}{2y} \int_{-y}^y \frac{1}{D(\zeta)} d\zeta.$$

Since $D(y)$ is a periodic function with period $p = 2\pi$, we can compute the harmonic mean as

$$\langle D^{-1} \rangle = \frac{1}{2\pi} \int_0^{2\pi} D(\zeta) d\zeta.$$

Expressing the approximate solution (1.21) in terms of the original variable x , we have

$$K_0(x) = \frac{1}{D(\omega x)} \frac{1}{2\sqrt{\langle D^{-1} \rangle}} \exp^{-|x-\xi|\sqrt{\langle D^{-1} \rangle}}. \quad (1.22)$$

This expression shows the exponential decay of the amplitude of the oscillations, and reveals the frequency of the oscillations.

A property of a dispersal kernel is that $\int_{-\infty}^{\infty} K(x) dx = 1$, Since $K_0(x)$ is an approximation to the true kernel, it may not satisfy this property. To circumvent this problem we can normalize the approximate solution in order to sum a unity.

Figure 1.8 shows the normalized approximate solution (1.22) and the numerical solution. The approximation gives a very accurate representation to the numerical solution of the dispersal kernel equation.

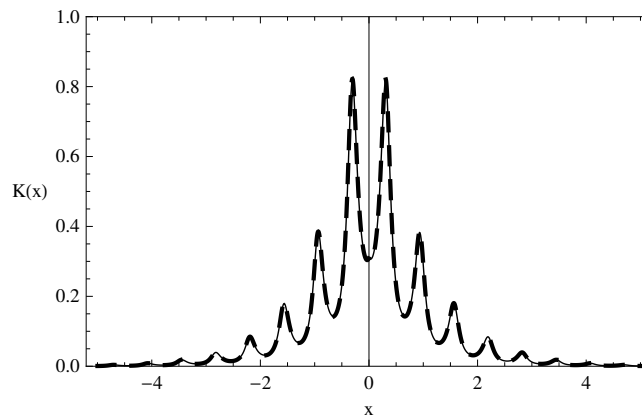


Figure 1.8: Numerical solution (continuous line) and Approximated solution (dashed line) to the Dispersal Kernel equation. Parameters used: $\omega = 10$; $\gamma = 0, 35$; Diffusion function: $D(\omega x) = \frac{1}{2} \sin(\omega x + \frac{\pi}{2}) + \frac{1}{2} + \gamma$.

2D Dispersal Kernel Approximation

For the 2D model, we also assume a positive periodic diffusion function, that is, $D(\mathbf{x} + \mathbf{x}_p) = D(\mathbf{x})$, where $\mathbf{x} = (x_1, x_2)$ and $\mathbf{x}_p = (x_{1p}, x_{2p})$ is a periodic vector denoting with x_{1p} and x_{2p} the periodicity of the components x_1 and x_2 respectively.

We follow the same spatial scale analysis as the 1D model, where the oscillations of the solution take place at the small scale, and the exponential decay of the amplitude be the large scale. Let $\omega = \max\{x_{1p}, x_{2p}\}$, and let the small parameter $\epsilon = 1/\omega$ with $\omega > 1$. We define the new independent scale variables

$$\mathbf{y} = \frac{\mathbf{x}}{\epsilon}, \quad \mathbf{x} = \mathbf{x}. \quad (1.23)$$

Here too, variations of order $\mathcal{O}(1)$ in the fast variable, \mathbf{y} , become small variations of order $\mathcal{O}(\epsilon)$ in the slow variable \mathbf{x} . Introducing the scale variables in the dispersal kernel equation (1.13), the derivatives transform, with $\nabla \rightarrow \nabla_x + \frac{1}{\epsilon}\nabla_y$, and $\nabla^2 = \nabla \cdot \nabla \rightarrow \nabla_x^2 + \frac{2}{\epsilon}\nabla_x\nabla_y + \frac{1}{\epsilon^2}\nabla_y^2$, where the subscripts denote the variable being differentiate (see Appendix B and Garlick et al., 2011 for details). The dispersal kernel equation in the new scale variables becomes then

$$(\nabla_x^2 + \frac{2}{\epsilon}\nabla_x\nabla_y + \frac{1}{\epsilon^2}\nabla_y^2)(D(\mathbf{y})K) - K = \delta(\mathbf{x} - \xi). \quad (1.24)$$

With the scale variables the diffusion function $D(\mathbf{y})$ has a period vector $\mathbf{y}_p = (y_{1p}, y_{2p})$. Now we assume a regular asymptotic expansion for K of the form

$$K \sim K_0(\mathbf{x}, \mathbf{y}) + \epsilon K_1(\mathbf{x}, \mathbf{y}) + \epsilon^2 K_2(\mathbf{x}, \mathbf{y}) + \dots, \quad (1.25)$$

and substitute into equation (1.24). The first term approximation of the solution of the partial differential equation (1.24) is given by (see Appendix B for details)

$$K_0(\mathbf{x}, \mathbf{y}) = \frac{1}{D(\mathbf{y})} \frac{\langle D^{-1} \rangle}{2\pi} K_o\left(\langle D^{-1} \rangle \|\mathbf{x} - \xi\|\right), \quad (1.26)$$

where K_o is the modified Bessel function of order zero, and $\langle D^{-1} \rangle$ is the harmonic mean of the diffusion over the whole domain \mathbf{R}^2 . Since the diffusion is a positive and periodic function, with period $\mathbf{y}_p = (y_{1p}, y_{2p})$, the harmonic mean can be computed by

$$\langle D^{-1} \rangle = \frac{1}{A} \int_0^{y_{1p}} \int_0^{y_{2p}} \frac{1}{D(\mathbf{y})} dy_{2p} dy_{1p}, \quad (1.27)$$

where A is the area of the rectangle $y_{1p} \times y_{2p}$. Returning to the original variables the approximate solution (1.28) is given by

$$K_0(\mathbf{x}) = \frac{1}{D(\mathbf{x}/\epsilon)} \frac{\langle D^{-1} \rangle}{2\pi} K_o \left(\langle D^{-1} \rangle \|\mathbf{x} - \xi\| \right). \quad (1.28)$$

Figure 1.9 shows the approximated and numerical solution to the dispersal kernel equation in 2D. Here again, we can see the accurate approximation to the numerical solution.

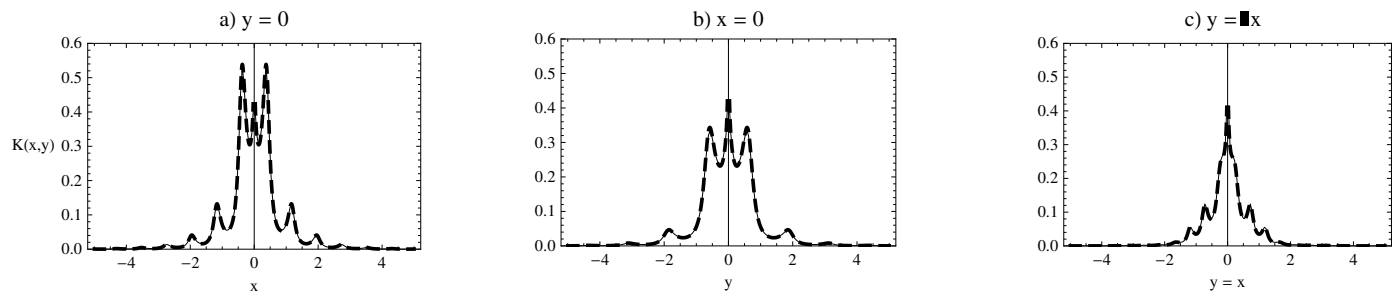


Figure 1.9: Numerical solution (continuous line) and Approximated solution (dashed line) to the Dispersal Kernel equation. Parameters used: $\omega = (8, 5)$; $\gamma = 0, 35$; Diffusion function: $D(\omega x) = \frac{1}{2} \sin(8x + \frac{\pi}{2}) \sin(5x + \frac{\pi}{2}) + \frac{1}{2} + \gamma$.

1.4 Discussion

The Model

Frequently, the seed shadow generated by animals, does not decline in a monotonous way from seed source. For fleshy fruit plants dispersed by birds, a spatial pattern of seed rain emerges at a certain spatial scale (Kollmann, 2000). Seeds are not dispersed in a randomly way, on the contrary, seeds follow animal movements and are deposited with a higher probability at specific places, where the animal tends to settle. The settling site may be perches, feeding roosts, latrines, some specific habitats like forest gaps, etc. The feeding and movement behavior of the disperser result in an aggregated spatial distribution of seeds .

Animal seed dispersal models are less developed than wind dispersal (Levin et al., 2003; Nathan and Muller-Landau, 2000). Models for describing seed shadows generated by animals, combine data on animal's mean and rate of displacement and seed passage times (Levin et al., 2003). These models provide frequency histograms of seed density against distance (Murray, 1988; Westcott et al., 2005). Some of them fit various statistical distributions to accommodate the multimodality of the seed distribution (Russo et al., 2006). Although these attempts describe the heterogeneous and multimodal pattern of seed distribution, they lack a general and theoretical framework for the understanding of the observed patterns.

Diffusion and settling models are theoretical models that have been used for deriving dispersal kernels (Okubo and Levin, 2001; Neubert et al., 1995; Powell and Zimmermann, 2004). They are simple and flexible to incorporate animal movements, animal behavior and seed passage rates.

Diffusion and settling models may be a good theoretical framework to develop simple models for animal dispersed seeds. Despite of the simplicity of the model, few authors have attempted to use it for modelling animal seed dispersal. Our proposed model belongs to these type of models. It incorporates general animal movements through the diffusion approximation of uncorrelated random walks in a heterogeneous, yet periodic, environment, and takes a constant rate of seed passage. The proposed model is able to reproduce the clumping pattern observed under field conditions, showing peaks of seed densities at sites where the dispersers tend to settle (high residence time). Although, the heterogeneous environment used in the model is hypothetical, it shows the aggregation of seeds under the settling sites. Powell's model for seed dispersal by animal cashers, uses Fickian diffusion and a settling probability which depends on the spatial location. His model also shows the aggregated pattern of seed distribution, but the multi-scale and homogenization approximation loses the heterogeneity (Powell and Zimmermann, 2004).

Developing more realistic models under diffusion and settling model framework, certainly provides a theoretical perspective to analyze the process behind the observed pattern of seed dispersal by animals. Furthermore, it may provide other types of distributions other than the traditionally used, distributions that capture the observed field patterns.

Multiple Scales and Homogenization Technique

One of the main purposes of a seed dispersal model is to derive a dispersal kernel for modelling plant dispersal. An analytical expression for the dispersal kernel is always desired, but may be difficult to obtain. A numerical solution to the dispersal kernel model can serve for the purpose of modelling plant dispersal, nonetheless an analytical expression may have advantages computationally and for further analytical analysis. Analytical solutions are frequently unavailable, but an attempt to derive an analytical approximation is always recommended.

Perturbation methods are techniques to derive analytical approximation to differential equations (Holmes, 1995). For our model we applied a multiple scales and homogenization technique to derive an analytical approximation to the dispersal kernel. This technique proved to be suitable for our model, since the approximation retained the heterogeneity of the environment, a feature we wanted to preserve in the dispersal kernel. This characteristic is due to the type of diffusion we used to model animal movement. The diffusion approximation of the uncorrelated random walk is referred as ecological diffusion ($\nabla^2(D(\mathbf{x}), K(\mathbf{x}))$) (Turchin, 1998; Okubo and Levin, 2001). When applying homogenization technique to ecological diffusion, the approximated solution preserves the fast variable, which describes the environmental heterogeneity (Garlick et al., 2011), contrary to Fickian diffusion ($\nabla(D(\mathbf{x})\nabla K(\mathbf{x}))$), in which the process of homogenization soothes the heterogeneity of the environment.

Powell and Zimmermann (2004) modeled animal seed dispersal using Fickian diffusion, and applied multiple scales and homogenization techniques in order to derive an analytical expression for the kernel. The resulting kernel did not preserved the heterogeneity of the diffusion function. On the other hand, Garlick et al. (2011), modeled dispersal of chronic wasting disease by mule deer, using ecological diffusion in a two dimension space. The approximated solution obtained, when applied

homogenization technique, preserved the environmental heterogeneity. Besides the advantage of retaining the heterogeneity, homogenization applied to ecological diffusion in multiple dimensions is much simpler as Fickian diffusion.

Behavior of the Dispersal Kernel

The behavior of the dispersal kernel derived by our model is determined by two parameters. These parameters represent the distance between settling sites and the residence time at those sites. The distance between settling sites determines the heterogeneity of the seed shadow. The smaller the distance the more difference in seed density between settling sites and the space between them. This is reasonable, since the less spaced settling sites, the greater the opportunity of the disperser to reach a settling site before dropping or defecating the seed on the way. On the other hand, more space between settling sites, increases the probability of the seed to be deposited in between. This generates a wider dispersion around the settling sites, which makes less heterogeneous the seed shadow.

Now, the residence time of the dispersers at the settling sites, determines how far a seed may travel. For greater residence times, the majority of seeds are dispersed around the source. The longer the time the disperser spends at the settling site, increases the probability of dropping the seed there. This means that with longer residence times, the seeds are dispersed with higher probability to the nearby perches, feeding roosts, latrines, etc. Conversely, if the disperser behaves with a high motility, and does not stop for long time at the settling sites, the probability of a seed to be dispersed longer distances is higher. This generates a dispersal kernel with a fatter tail. In other words, the smaller the residence time, the further the seed may be dispersed. This may have implications on the rate of plant expansion.

1.5 Conclusions

We consider that diffusion and settling models could be a general framework for developing animal seed dispersal models. From simple and general assumptions on animal movements and seed passage time, the model was able to reproduce the aggregated spatial pattern of animal dispersed seeds. More realistic assumptions can be incorporated in the model to analyze and predict seed shadows. Furthermore, in some cases it may be possible to have approximated analytical solutions to the model, as is our case, a very desirable situation, for modeling plant dispersal.

Multiple scales and homogenization techniques proved to be suitable to treat ecological diffusion, since it retains the heterogeneity of the environment in the approximated solution. Furthermore, when modeling in a multiple-dimensions, the procedure of homogenization is much simpler than Fickian diffusion.

Finally, the parameters that determines the behavior of the dispersal kernel can be obtained experimentally, a chance to test the effectiveness of the model.

1.6 Appendix

1.6.1 Appendix A: Approximate solution to the 1D Dispersal Kernel Equation, using multiple scales and homogenization technique.

Case $\omega > 1$

The non-dimensional differential equation of the dispersal kernel in one dimension is given by

$$\frac{d^2}{dx^2} (D(x)K) - K = -\delta(x - \xi), \quad (1.29)$$

where $D(x)$ is the diffusion function, which we assume to have the following properties:

- i. $D(x)$ is a limited, positive and continuous function, so that $0 < D_{min} \leq D(x) \leq D_{max}$, $\forall x \in \mathbf{R}$.
- ii. $D(x)$ is a periodic function with period $x_p = 2\pi/\omega$, so that, $D(x + x_p) = D(x)$; where ω is the frequency.

A simple diffusion function satisfying the above assumption and that will be used through the analysis is

$$D(x) = \left[\frac{1}{2} \sin(\omega x + \pi/2) + \frac{1}{2} \right] + \gamma, \quad (1.30)$$

where $0 < \gamma < 1$ and ω is the frequency of oscillation. It can be verified that $D_{max} = 1 + \gamma$ and $D_{min} = \gamma$. For further analysis we may write explicitly the frequency in the diffusion's argument, $D = D(\omega x)$.

Two spatial scales can be distinguished from the numerical solution of the differential equation (1.29) (Figure 1.2)(see section Results). One fast scale, associated with the oscillations of the solution, which we assume to be of order $\mathcal{O}(1/\omega)$, and a slow scale of order $\mathcal{O}(1)$, which describes the decay of the amplitudes of the oscillations. We introduce the small parameter $\epsilon = 1/\omega$, which relates both scales. Let x be the slow scale variable, and $y = x/\epsilon$ the fast scale variable. Note that variations of order $\mathcal{O}(1)$ in the fast y variable, become small variations of order $\mathcal{O}(\epsilon)$ in the slow x variable.

Introducing the scale variables x and y into the differential equation (1.29), and treating them as independent, results in a partial differential equation of the unknown function $K(x, y)$. The spatial derivatives in (1.29) transform as follows (Holmes, 1995)

$$\frac{d}{dx} \rightarrow \frac{\partial}{\partial x} + \frac{1}{\epsilon} \frac{\partial}{\partial y}, \quad \frac{d^2}{dx^2} \rightarrow \frac{\partial^2}{\partial x^2} + \frac{2}{\epsilon} \frac{\partial}{\partial x} \frac{\partial}{\partial y} + \frac{1}{\epsilon^2} \frac{\partial^2}{\partial y^2}. \quad (1.31)$$

To simplify notation we use $\partial_x = \frac{\partial}{\partial x}$. The differential equation for the dispersal kernel after changing variables and multiplying by ϵ^2 becomes then,

$$(\partial_y^2 + 2\partial_y\partial_x + \epsilon^2\partial_x^2)(D(y)K) - \epsilon^2K = -\epsilon^2\delta(x - \xi), \quad (1.32)$$

Note that the diffusion $D(\omega x) = D(x/\epsilon)$, became $D(y)$ after changing variables, and has period $y_p = 2\pi$ in the fast variable. We assume that $K(x, y)$ is also y_p -periodic in the fast variable, this means that $K(x, y + y_p) = K(x, y)$. Moreover, if $K(x, y)$ is smooth enough, we must have $\partial_y K(x, y + y_p) = \partial_y K(x, y)$ (Holmes, 1995).

We now consider a regular asymptotic expansion for $K(x, y)$ of the form

$$K \sim K_0(x, y) + \epsilon K_1(x, y) + \epsilon^2 K_2(x, y) + \dots \quad (1.33)$$

Substituting this expansion in (1.32) and collecting terms, we obtain the following equations

$\mathcal{O}(1)$:

$$\partial_y^2(D(y)K_0) = 0 \quad (1.34)$$

whose general solution is

$$K_0(x, y) = \frac{a_0(x)}{D(y)}y + \frac{b_0(x)}{D(y)}, \quad (1.35)$$

where $a_0(x)$ and $b_0(x)$ are coefficient functions to be determined. Considering the periodic assumption on the fast variable we must have $a_0(x) = 0$, hence

$$K_0(x, y) = \frac{b_0(x)}{D(y)}. \quad (1.36)$$

$\mathcal{O}(\epsilon)$:

$$\partial_y^2(D(y)K_1) + 2\partial_y\partial_x(D(y)K_0) = 0. \quad (1.37)$$

Substituting $K_0(x, y)$ in the above equation yields

$$\partial_y^2(D(y)K_1) = 0, \quad (1.38)$$

since

$$\partial_y \partial_x (D(y)K_0) = \partial_y \partial_x \left(D(y) \frac{b_0(x)}{D(y)} \right) = \partial_y \partial_x (b_0(x)) = 0.$$

Considering again the periodic assumption of $K(x, y)$ in the fast variable, the general solution to the differential equation of order $\mathcal{O}(\epsilon)$, is then

$$K_1(x, y) = \frac{b_1(x)}{D(y)}, \quad (1.39)$$

where $b_1(x)$ is a coefficient function to be determined.

$\mathcal{O}(\epsilon^2)$:

$$\partial_y^2 (D(y)K_2) + 2\partial_y \partial_x (D(y)K_1) + \partial_x^2 (D(y)K_0) - K_0 = -\delta(x - \xi). \quad (1.40)$$

When substituting the expressions of $K_0(x, y)$ and $K_1(x, y)$ in the above equation, the second and third term of the left hand of the equation become zero and $\partial_x^2 b_0(x)$ respectively, as shown below

2nd. term:

$$\partial_y \partial_x (D(y)K_1) = \partial_y \partial_x \left(D(y) \frac{b_1(x)}{D(y)} \right) = \partial_y \partial_x (b_1(x)) = 0, \quad (1.41)$$

3th. term:

$$\partial_x^2 (D(y)K_0) = \partial_x^2 \left(D(y) \frac{b_0(x)}{D(y)} \right) = \partial_x^2 b_0(x) = b_0''(x) \quad (1.42)$$

where we wrote $\partial_x^2 b_0(x) = b_0''(x)$. The $\mathcal{O}(\epsilon^2)$ differential equation can be written as

$$\partial_y^2 (D(y)K_2) + b_0''(x) - \frac{b_0(x)}{D(y)} = -\delta(x - \xi), \quad (1.43)$$

or equivalently

$$\partial_y^2 (D(y)K_2) = -b_0''(x) + \frac{b_0(x)}{D(y)} - \delta(x - \xi). \quad (1.44)$$

The unknown coefficient function $b_0(x)$ appears in the $\mathcal{O}(\epsilon^2)$ differential equation. In order to solve for $b_0(x)$, we homogenized the equation (1.44) by averaging each term in the fast variable over a period $y_p = 2\pi$ (Holmes 1995, Garlick et al. 2011). The average of a function $v(x)$ over an interval $[a, b]$ is defined as

$$\langle v \rangle = \frac{1}{b-a} \int_a^b v(x) dx.$$

Averaging the equation (1.44) over a period $y_p = 2\pi$, and using the fundamental theorem calculus we have

$$\left\langle \partial_y^2(D(y)K_2) \right\rangle = \frac{1}{2\pi} \int_0^{2\pi} \partial_y^2(D(y)K_2) = \partial_y(D(y)K_2) \Big|_0^{2\pi} = 0, \quad (1.45)$$

where the periodic assumption on K and D has been considered ($\partial_y(D(y+y_p)K(x, y+y_p)) = \partial_y(D(y)K(x, y))$). The other averaged terms are as follows

$$\langle b_0''(x) \rangle = b_0''(x) \quad (1.46)$$

$$(1.47)$$

$$\langle \delta(x - \xi) \rangle = \delta(x - \xi)$$

$$(1.48)$$

$$\left\langle \frac{b_0(x)}{D(y)} \right\rangle = b_0(x) \frac{1}{2\pi} \int_0^{2\pi} \frac{1}{D(y)} dy.$$

We define $\langle D^{-1} \rangle = \frac{1}{2\pi} \int_0^{2\pi} \frac{1}{D(y)} dy$, which represents the harmonic mean of the diffusion. Note that $\langle D^{-1} \rangle$ is a constant. With the averaged terms the homogenized differential equation to (1.44) is given by

$$b_0''(x) - \langle D^{-1} \rangle b_0(x) = -\delta(x - \xi). \quad (1.49)$$

We use the Fourier Transform method to solve the homogenized equation. First we make a change of variables $\zeta = x - \xi$, and then apply the Fourier Transform and its derivative properties, yielding

$$-k^2 F\{b_0(\zeta + \xi)\} - \langle D^{-1} \rangle F\{b_0(\zeta + \xi)\} = -F\{\delta(\zeta)\},$$

or

$$-(k^2 + \langle D^{-1} \rangle) F\{b_0(\zeta + \xi)\} = -\frac{1}{\sqrt{2\pi}},$$

$$F\{b_0(\zeta + \xi)\} = \frac{1}{\sqrt{2\pi} (k^2 + \langle D^{-1} \rangle)}.$$

Applying the Fourier Inverse to the above equation we have

$$b_0(\zeta + \xi) = \frac{1}{\sqrt{2\langle D^{-1} \rangle}} \exp^{-|\zeta|\sqrt{2\langle D^{-1} \rangle}}.$$

Returning to the original variable, we arrive at the solution of the homogenized differential equation

$$b_0(x) = \frac{1}{2\sqrt{\langle D^{-1} \rangle}} \exp^{-|x-\xi|\sqrt{\langle D^{-1} \rangle}}.$$

Knowing the coefficient function $b_0(x)$ we have the first term approximation to the solution of the dispersal kernel equation which is

$$K_0(x, y) = \frac{1}{D(y)} \frac{1}{2\sqrt{\langle D^{-1} \rangle}} \exp^{-|x-\xi|\sqrt{\langle D^{-1} \rangle}},$$

so that $K \sim K_0 + \mathcal{O}(\epsilon)$.

1.6.2 Appendix B: Approximate solution to the Dispersal Kernel in 2 dimensions, using multiple scales and homogenization techniques.

The non-dimensional differential equation of the dispersal kernel in two dimensions (\mathbf{R}^2) is given by

$$\nabla^2(D(\mathbf{x})K) - K = -\delta(\mathbf{x} - \xi), \quad (1.50)$$

where $\mathbf{x} \in \mathbf{R}^2$, $\mathbf{x} = (x_1, x_2)$ and $D(\mathbf{x})$ is the diffusion function, which we assume to have the following properties:

- i. $D(\mathbf{x})$ is a limited, positive and smooth function, so that $0 < D_{min} \leq D(\mathbf{x}) \leq D_{max}$, $\forall \mathbf{x} \in \mathbf{R}^2$.
- ii. $D(\mathbf{x})$ is a periodic function with period x_p . This means, there is a period vector $x_p = (2\pi/\omega_1, 2\pi/\omega_2)$, so that $D(\mathbf{x} + \mathbf{x}_p) = D(\mathbf{x})$; where $\omega_1 > 1$ and $\omega_2 > 1$ are the frequencies of oscillations in the coordinates x_1 and x_2 respectively.

A diffusion function satisfying the above assumption may be $D(\mathbf{x}) = \frac{1}{2} \sin(\omega_1 x_1) \sin(\omega_2 x_2) + \frac{1}{2} + \gamma$, $\gamma > 0$. In this case, the period vector is $x_p = (2\pi/\omega_1, 2\pi/\omega_2)$. The periodicity implies that if we know the values of the function in the rectangle $a \leq x_1 \leq a + 2\pi/\omega_1$ and $b \leq x_2 \leq 2\pi/\omega_2$, where a and b are arbitrary in the domain, then we can determine the diffusion function everywhere. We define the frequency vector $\omega = (\omega_1, \omega_2)$, and for further analysis, we write the frequency in a explicit way in the diffusion's argument, $D = D(\omega\mathbf{x})$.

For the 2D dispersal kernel equation, we proceed with the same spatial analysis as in the 1D equation, assuming a fast spatial scale variable associated with the oscillations, and a slow variable describing the decay of the amplitudes. Let $\omega_{max} = \max\{\omega_1, \omega_2\}$, and define $\epsilon = 1/\omega_{max}$. Let \mathbf{x} be the slow scale variable and $\mathbf{y} = \mathbf{x}/\epsilon$. Introducing these scale variables into the differential equation (1.50), the unknown function becomes $K(\mathbf{x}, \mathbf{y})$, and following ? and Garlick et al. (2011) the derivatives transform as follows

$$\begin{aligned}\nabla &\rightarrow \nabla_x + \frac{1}{\epsilon}\nabla_y, \\ \nabla \cdot \nabla &\rightarrow (\nabla_x + \frac{1}{\epsilon}\nabla_y) \cdot (\nabla_x + \frac{1}{\epsilon}\nabla_y) \rightarrow \nabla_x^2 + \frac{2}{\epsilon}\nabla_x \nabla_y + \frac{1}{\epsilon^2}\nabla_y^2.\end{aligned}$$

where the subscript is the derivative of the variable being differentiated. Substituting the derivatives and the unknown function in equation (1.50), and after multiplying by ϵ^2 , yields

$$(\nabla_y^2 + 2\epsilon\nabla_y \nabla_x + \epsilon^2\nabla_x^2)(D(\mathbf{y})K) - \epsilon^2 K = -\epsilon^2 \delta(\mathbf{x} - \xi). \quad (1.51)$$

Note that the diffusion function depends only on the fast variable \mathbf{y} , with oscillations of period $\mathbf{y}_p = (y_{1p}, y_{2p})$ where $y_{1p} = \omega_{max}(2\pi/\omega_1)$ and $y_{2p} = \omega_{max}(2\pi/\omega_2)$. We make the assumption that $K(\mathbf{x}, \mathbf{y})$ is also \mathbf{y}_p -periodic in the fast variable, this means $K(\mathbf{x}, \mathbf{y} + \mathbf{y}_p) = K(\mathbf{x}, \mathbf{y})$, and that $\nabla_y K(\mathbf{x}, \mathbf{y} + \mathbf{y}_p) = \nabla_y K(\mathbf{x}, \mathbf{y})$.

Considering a regular asymptotic expansion for $K(\mathbf{x}, \mathbf{y})$ of the form

$$K(\mathbf{x}, \mathbf{y}) = K_0(\mathbf{x}, \mathbf{y}) + \epsilon K_1(\mathbf{x}, \mathbf{y}) + \epsilon^2 K_2(\mathbf{x}, \mathbf{y}) + \dots \quad (1.52)$$

Substituting this expansion into (1.51), and collecting terms in ϵ , we obtain the following equations:

$\mathcal{O}(1)$:

$$\nabla_y^2(D(\mathbf{y})K_0) = 0,$$

whose general solution is

$$K_0(\mathbf{x}, \mathbf{y}) = \frac{a_0(\mathbf{x})}{D(\mathbf{y})}\mathbf{y} + \frac{b_0(\mathbf{x})}{D(\mathbf{y})},$$

where $a_0(\mathbf{x})$ and $b_0(\mathbf{x})$ are coefficient functions to be determined. Considering the assumption that $K(\mathbf{x}, \mathbf{y})$ is periodic in the fast variable, we must have $a_0(\mathbf{x}) = 0$, this leads to the solution

$$K_0(\mathbf{x}, \mathbf{y}) = \frac{b_0(\mathbf{x})}{D(\mathbf{y})}. \quad (1.53)$$

$\mathcal{O}(\epsilon)$:

$$\nabla_y^2(D(\mathbf{y})K_1) + 2\epsilon\nabla_y\nabla_x(D(\mathbf{y})K_0) = 0. \quad (1.54)$$

Substituting K_0 in the above equation and simplifying ($\nabla_y\nabla_x(D(\mathbf{y})K_0) = 0$), we get

$$\nabla_y^2(D(\mathbf{y})K_1) = 0. \quad (1.55)$$

Using the periodic condition in the fast variable of $K(\mathbf{x}, \mathbf{y})$, the general solution of the equation above, is

$$K_1(\mathbf{x}, \mathbf{y}) = \frac{b_1(\mathbf{x})}{D(\mathbf{y})}, \quad (1.56)$$

where $b_1(\mathbf{x})$ is a coefficient function to be determined.

$\mathcal{O}(\epsilon^2)$:

$$\nabla_y^2(D(\mathbf{y})K_2) + 2\nabla_y\nabla_x(D(\mathbf{y})K_1) + \nabla_x(D(\mathbf{y})K_0) - K_0 = -\delta(\mathbf{x} - \xi). \quad (1.57)$$

Substituting (1.53) and (1.56) into (1.58) and simplifying ($\nabla_y\nabla_x(D(\mathbf{y})K_1) = 0$ and $\nabla_x^2((D(\mathbf{y})K_0) = \nabla_x^2(b_0(\mathbf{x}))$) yields

$$\nabla_y^2(D(\mathbf{y})K_2) + \nabla_x^2((D(\mathbf{y})K_0) - \frac{b_0(\mathbf{x})}{D(\mathbf{y})}) = -\delta(\mathbf{x} - \xi),$$

or

$$\nabla_y^2(D(\mathbf{y})K_2) = -\nabla_x^2(b_0(\mathbf{x})) + \frac{b_0(\mathbf{x})}{D(\mathbf{y})} - \delta(\mathbf{x} - \xi). \quad (1.58)$$

The unknown coefficient function $b_0(\mathbf{x})$ appears in the differential equation above. In order to solve for $b_0(\mathbf{x})$, we proceed to homogenized the equation (1.58) by averaging each term in relation to the fast variable. Note that the diffusion $D(\mathbf{y})$ depends only on the fast variable, with a period vector $\mathbf{y}_p = (y_{1p}, y_{2p})$. Let $\Omega_p = [0, y_{1p}] \times [0, y_{2p}]$, and $|\Omega_p|$ be its area. Now we proceed to average the equation over the region Ω , starting with the term on the left hand of the equation, and using the divergence theorem and periodic conditions on the functions $D(\mathbf{y})$ and $K(\mathbf{x}, \mathbf{y})$ we have

$$\langle \nabla_y^2 (D(\mathbf{y})K_2) \rangle = \frac{1}{|\Omega|} \int_{\Omega} \nabla_y^2 (D(\mathbf{y})K_2) d\Omega = \frac{1}{|\Omega|} \int_{\partial\Omega} \nabla_y (D(\mathbf{y})K_2) \cdot \mathbf{n} dS = 0 \quad (1.59)$$

where $\partial\Omega$ is the border of the region Ω and $\hat{\mathbf{n}}$ is the outward unitary normal vector of Ω . Averaging the right hand terms of equation (1.58)

$$\langle \nabla b_0(\mathbf{x}) \rangle = \nabla b_0(\mathbf{x}) \quad (1.60)$$

$$\langle \delta(\mathbf{x} - \xi) \rangle = \delta(\mathbf{x} - \xi) \quad (1.61)$$

$$\left\langle \frac{b_0(\mathbf{x})}{D(y)} \right\rangle = b_0(\mathbf{x}) \frac{1}{|\Omega|} \int_{\Omega} \frac{1}{D(\mathbf{y})} d\Omega. \quad (1.62)$$

We define $\langle D^{-1} \rangle$ as

$$\langle D^{-1} \rangle = \frac{1}{|\Omega|} \int_{\Omega} \frac{1}{D(\mathbf{y})} d\Omega = \frac{1}{y_{1p} \times y_{2p}} \int_0^{y_{1p}} \int_0^{y_{2p}} \frac{1}{D(y_1, y_2)} dy_2 dy_1.$$

Note that $\langle D^{-1} \rangle$ is a constant, and does not depend on the fast variable anymore. After averaging terms we arrive at the homogenized differential equation of (1.58)

$$\nabla^2 b_0(\mathbf{x}) - \langle D^{-1} \rangle b_0(\mathbf{x}) = -\delta(\mathbf{x} - \xi) \quad (1.63)$$

The differential equation above is a modified Helmholtz equation. For, $r = \sqrt{(x_1 - \xi_1)^2 + (x_2 - \xi_2)^2} > 0$, (1.63) transforms into

$$\frac{d^2}{dr^2} K(r) - \frac{1}{r} \frac{d}{dr} K(r) - \langle D^{-1} \rangle K(r) = 0, \quad (1.64)$$

whose general solution is given by

$$K(r) = AI_o(\sqrt{\langle D^{-1} \rangle} r) + BK_o(\sqrt{\langle D^{-1} \rangle} r), \quad (1.65)$$

where I_o and K_o are the modified Bessel functions of order zero, A and B are constants to be determined. Here we introduce a natural condition for the dispersal kernel, $\lim_{r \rightarrow \infty} K(r) = 0$, thus we must have $A = 0$, since $I_o(r)$ is unbounded as $r \rightarrow \infty$, this leads to the following solution,

$$K(r) = BK_o(\sqrt{\langle D^{-1} \rangle} r). \quad (1.66)$$

In order to determine the constant B , we apply the Green's function property of discontinuity $\lim_{\epsilon \rightarrow 0} \int_{C_\epsilon} -\frac{\partial K}{\partial \mathbf{n}} ds = 1$, where c_ϵ is a small circle with radius ϵ centered at (ξ_1, ξ_2) ,

$$\lim_{\epsilon \rightarrow 0} \int_{C_\epsilon} -\frac{\partial K}{\partial \mathbf{n}} ds = \lim_{\epsilon \rightarrow 0} \int_{C_\epsilon} -B \frac{\partial K_o}{\partial r} ds = \lim_{\epsilon \rightarrow 0} \int_0^{2\pi} -\epsilon B \frac{\partial K_o}{\partial r} d\theta = 1.$$

Asymptotically, $K_o(\sqrt{\langle D^{-1} \rangle} r) \sim \ln(1/\sqrt{\langle D^{-1} \rangle} r)$ as $r \rightarrow 0$, so we may have from the above limit

$$\lim_{\epsilon \rightarrow 0} \int_0^{2\pi} -\epsilon B \frac{\partial K_o}{\partial r} d\theta = 1 \quad (1.67)$$

$$(1.68)$$

$$\lim_{\epsilon \rightarrow 0} -2\pi \epsilon B \frac{\partial K_o}{\partial r} \Big|_{r=\epsilon} = 1 \quad (1.69)$$

$$\lim_{\epsilon \rightarrow 0} 2\pi \epsilon B \frac{1}{\epsilon \sqrt{\langle D^{-1} \rangle}} = 1 \quad (1.70)$$

$$B = \frac{\sqrt{\langle D^{-1} \rangle}}{2\pi},$$

hence the first term approximation to the solution for the dispersal kernel equation in 2D is

$$K_0(\mathbf{x}, \mathbf{y}) = \frac{1}{D(\mathbf{y})} \frac{\sqrt{\langle D^{-1} \rangle}}{2\pi} K_o\left(\sqrt{\langle D^{-1} \rangle} r\right),$$

or in $\mathbf{x} = (x_1, x_2)$ coordinates,

$$K_0(\mathbf{x}) = \frac{1}{D(\mathbf{x}/\epsilon)} \frac{\sqrt{\langle D^{-1} \rangle}}{2\pi} K_o\left(\sqrt{\langle D^{-1} \rangle} \|\mathbf{x} - \xi\|\right). \quad (1.71)$$

Capítulo 2

Invasão Biológica de uma planta de fruto carnosos dispersada por pássaros e sujeita a efeito Allee

Biological Invasion of a fleshy fruited plant dispersed by birds and subject to Allee effect

Abstract. We use an integro-difference equation to model the dispersal of a fleshy fruited plant dispersed by birds and subject to Allee effect. We developed the model in three steps: a) the population growth model with Allee effect, b) development of the dispersal kernel, and c) the dispersal process. The dispersal kernel showed the clumping distribution characterized by the seed rain generated by frugivores birds under field conditions. The clumping pattern reflects the heterogeneity of the environment which influences the animals' movement. The model showed a pulsed invasion behavior, contrary to a continuous and constant expansion. The pulsed invasion behavior was characterized by front population stasis or stagnation followed by a jump or step advance. This behavior was observed for strong intensities of Allee effect, but for subtle intensities, the front population advanced at a roughly constant rate. For the expansion speed, we homogenized the dispersal kernel, which yielded good approximations to the average expansion speeds.

2.1 Introduction

Plant population growth and seed dispersal are two major biological factors that determine the success of an invasion and its expansion rate. Any factor (physical or biological) that influences these two biological processes, alters the invasion dynamics. Biological or physical interactions

are constantly modifying the population growth and seed dispersal of plants, and thus leading to different invasion dynamics.

The Allee effect, from a demographic point of view, is a density-dependent effect, in which the per capita growth rate of the population is increased with the population density (Stephens et al., 1999). It mainly occurs at low population densities. At high densities, the Allee effect may not be significant in comparison with the negative effect of the intraspecific competition. One of the most documented factors that may induce an Allee effect in sexual populations, is mate finding (Boukal and Berec, 2002). At low population densities, the probability of finding mates may be too low, so that the population experiences a low per capita growth rate. The growth rate may be sometimes too low, that is insufficient to maintain the population, and eventually the population goes extinct. Here, an increase in the number of individuals, may rise the mate finding probability, avoiding population extinction. In sexual populations, the Allee effect due to mate finding, may be always present.

The Allee effect may be present whenever a sexual population experiences low densities. From a biological invasion perspective, this may occur at the initial stages of the invasion or at the front of it. Thus, Allee effect, has been considered lately when studying biological invasions of sexual populations, since it has profound effects on the invasion dynamics Taylor and Hastings (2005). One of the main effects is establishing colonization threshold for a successful invasion, and reducing expansion speeds (Lewis and Kareiva, 1993; Kot et al., 1996; Davis et al., 2004). It may be responsible for the lag phases observed in some plant invasions (Parker, 2004; Taylor and Hastings, 2005), and also for pattern formations (Petrovskii et al., 2002; Mistro et al., 2012).

Allee effect has been reported in plants and may be not an uncommon situation (Groom, 1998). Davis et al. (2004) detected an Allee effect, due to pollen limitation, at the front of an invasion of *Spartina alterniflora*. Following (Davis et al., 2004) findings, we propose an integro-difference (IDE) model for the study of an invasive plant subject to an Allee effect due to pollen limitations. The IDE model couples population growth and dispersal.

The spatial distribution of seeds dispersed is often summarized in a probability distance distribution, which is referred as the dispersal kernel. The seed production of an individual plant multiplied by its dispersal kernel is known as the the plant's seed shadow. Functional forms are fitted to dispersal data to describe the seed density distributions. It is suggested that the entire seed distribution (the local distribution and the tail) is important in determining the expansion speed of a plant (Levin et al., 2003).

As for the dispersal process, the dispersal syndrome (ornithochory, anemochory, barochory, etc.) a plant relies on to disperse its seeds, certainly influences the rate of the plant's expansion. Plants dispersed by birds or monkeys may have greater mean dispersal distance than wind dispersed seed plants (Clark et al., 2005), and this may result in a greater expansion rate (Kot et al., 1996). Moreover different seed dispersal vectors shape in different forms the seed shadows of a plant species. For wind dispersed plants, a t-Student function or Gaussian distributions accommodates well the dispersal data for wind dispersed plants, while the seed distribution of an animal dispersed plants may be better represented by an inverse power law (Clark et al., 2005). The Gaussian,

inverse power law and the exponential are the functional forms that traditionally are used to fit seed dispersal data. These functions are unimodal and decline monotonically with distance from the source or modal location.

For fleshy fruited invasive plants, whose major dispersal agents are birds (Gosper et al., 2005), the seed distribution may not decline in a simple way from source (Kollmann, 2000). Instead the seed rain generated by birds is heterogeneous, with seed aggregations or clumps at particular sites (? , and reference there in). It is suggested that various distributions should be used in order to capture the multimodality of the seed distribution (Russo et al., 2006). The sites of seed aggregation or clumping depend on bird's behavior. These sites may be places where the bird settles to rest or to feed, for example different habitats within a plant community or landscape such as forest gaps, patches at different successional stages or some vegetation features such as clusters of shrubs or isolated trees which the birds uses as perches or roosts (Kollmann 2000, Gosper et al. 2005).

The landscape or habitat structure together with the animals' behavior may influence the seed deposition pattern of an animal dispersed plant. It is suggested to incorporate these elements in theoretical and mechanistical models to derive theoretical dispersal kernels (Clark et al., 2005), which may be used to model plant dispersal.

Modelling plant dispersal under the framework of integrodifference- equations (IDE), has gained popularity , because it is ideal for the plants' nonoverlapping generations and for the flexibility to incorporate different dispersal kernels (Kot et al., 1996; Kot, 1992; Neubert et al., 1995). The majority of IDE models for the dispersal of organisms assume a homogeneous environment, but models dealing with heterogeneous environments are beginning to appear (Kawasaki and Shigesada, 2007; Dewhurst and Lutscher, 2009). Some models introduce heterogeneity at the population growth, others at both the population growth and seed dispersal process, and some others just at the seed dispersal process . These models mainly assume a periodic heterogeneous environment of alternating favorable and unfavorable habitats. Powell and Zimmermann (2004) used IDE to model the expansion of a plant dispersed by animal cashers, where the cashing sites were periodically distributed in the landscape. Their approach of introducing landscape heterogeneity is different to the general assumption of good and bad habitats. The heterogeneity is introduced into the dispersal process and was the result of modelling the seed shadows generated by animal vectors. Here we follow a similar approach, we address to model the expansion of a plant, whose seeds are dispersed by frugivores birds, using IDE. We introduce the environmental heterogeneity at the seed dispersal process, since the seed rain generated by birds is affected by the landscape or habitat structure. The dispersal kernel used in our model should reflect the landscape structure and the birds' behavior of dispersing seeds. We aim to analyze the expansion speeds in relation to the landscape structure and the rate of animal movements. The influence of the Allee effect in the expansion rate is analyzed and discussed.

2.2 The model

The model couples a population growth and a dispersal dynamics of a fleshy fruited plant dispersed by birds. We consider a perennial plant without a seed bank, and with a well defined small reproductive season. For the model, we take the time from one reproductive season to the following as the generational time, and divided into 3 phases: i) plant growth, ii) reproduction and seed output and iii) seed dispersal.

The whole model was developed in two stages: a) the local population growth model, and b) the dispersal process.

2.2.1 Local Dynamics: growth, reproduction and seed output

The model for the growth, reproduction and seed output follows the below diagram:

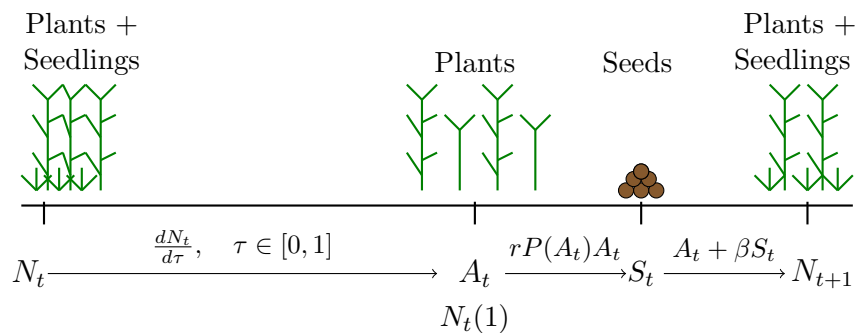


Figure 2.1: Diagram of the local population dynamics: growth, reproduction and seed output.

The different stages are described in the following section:

Growth Phase

Let n_t the population density at generation t , just after reproduction and seed establishment as seedlings. Hence, seedlings and the survivors of the past generation compose the population n_t . The growth phase begins with the recruitment of plants (seedlings) and ends just before the reproductive season. During this time, we assume that the population n_t is subject just to natural mortality and to a density dependent mortality, due to limited resources. We model the per capita rate of change of the density of plants n_t during the growth phase as follows:

$$\frac{1}{n_t(\tau)} \frac{dn_t}{d\tau} = -\mu_0 - \mu n_t, \quad (2.1)$$

where μ_0 is the mortality rate independent of the density, and μ is the mortality due to crowding effect. The variable τ represents the time of the growth phase, and we take $\tau = 0$ as the beginning and $\tau = 1$ as the end of the growth season. Solving the differential equation (2.1) with the initial condition $n_t(0) = n_t$, yields,

$$n_t(\tau) = \frac{n_t(0)}{e^{\tau\mu_0} + \frac{\mu}{\mu_0}(e^{\tau\mu_0} - 1)n_t(0)}. \quad (2.2)$$

From the above equation we have the population density right before the reproduction season ($\tau = 1$):

$$n_t(1) = \frac{n_t(0)}{e^{\mu_0} + \frac{\mu}{\mu_0}(e^{\mu_0} - 1)n_t(0)}, \quad (2.3)$$

which we may write as follows

$$n_t(1) = \frac{qn_t}{1 + cn_t}, \quad (2.4)$$

where,

$$q = e^{-\mu_0}, \quad c = \frac{\mu}{\mu_0}(1 - e^{-\mu_0}) \quad \text{and} \quad n_t(0) = n_t.$$

The parameter q represents the probability of survival the phase growth without crowding effect, and c measures the per capita susceptibility of crowding. If we scale the population density to the parameter c , and introduce the nondimensional density variables $N_t(1) = cn_t(1)$ and $N_t = cn_t$ we have the nondimensional model for the population growth phase

$$N_t(1) = \frac{qN_t}{1 + N_t}. \quad (2.5)$$

The population $N_t(1)$ is composed of the grown ups' seedlings and the adult survivors of the last generation. We may introduce the population $A_t = N_t(1)$ to represent the adult population, thus from (2.5) we have

$$A_t = \frac{qN_t}{1 + N_t}. \quad (2.6)$$

Reproductive phase and seed output

We assume a very short period of reproduction compared to the growth phase, and consider no mortality of the population during this period of time. Let γ be the proportion of mature plants in the population A_t , and let \hat{r} be the seeds produced per mature plant, so that the density of seeds produced by the mature plants (γA_t) is given by

$$S_t = \hat{r}\gamma A_t. \quad (2.7)$$

Here we will introduce the Allee effect. Following Davis et al. (2004) we consider an Allee effect due to pollen limitation, and that pollen availability is positively correlated with plant density. Since seed production depends on pollen availability, we assume that the number of seeds produced per plant depends on mature plant density $\hat{r}(\gamma A_t)$, and model seed density at generation t as follows,

$$S_t(A_t) = \hat{r}(\gamma A_t) \gamma A_t. \quad (2.8)$$

We use the rectangular hyperbola (RH) functional form for the per capita seed production $\hat{r}(\gamma A_t, \theta) = \hat{r} \frac{\gamma A_t}{\theta + \gamma A_t}$. The parameter θ is the density of mature plants, at which a mature plant can produce half of its total seed output. Substituting equation (2.5) for A_t into the seed production equation (2.8), and after some algebra yields

$$S_t(N_t) = r \left(\frac{N_t}{s + (s+1)N_t} \right) \frac{qN_t}{1 + N_t}, \quad (2.9)$$

where $s = \frac{\theta}{\gamma q}$ and $r = \hat{r}\gamma$. The parameter s is the parameter θ scaled to the mature plants survivors, and measures the strength of the Allee effect due to pollen limitation.

The population density after the growth phase is A_t , and the seeds produced by the mature plants of the growth phase is S_t . Let β be the probability of a seed become a seedling. From equations (2.5) and (2.8) we have the population density at the generation $t + 1$ given by

$$N_{t+1} = A_t + \beta S_t(A_t), \quad (2.10)$$

or in terms of the population density N_t we have

$$N_{t+1} = \left(1 + \frac{rN_t}{s + (s+1)N_t} \right) \frac{qN_t}{1 + N_t}. \quad (2.11)$$

2.2.2 Spatial Dynamics: Seed dispersal

After the plants have set their seeds, the seed dispersal process redistributes the seeds in space. We model the dispersal process in a one dimensional infinite space. For the dispersal process we introduce a dispersal kernel $K(x, y)$, as a density function (PDF) which describes the probability of a seed from a point x to be dispersed a distance $|x - y|$ to the location y . As a PDF, the dispersal kernel satisfies the property $K(z) > 0$ and $\int_{-\infty}^{\infty} K(z) dz = 1$. The seeds after the dispersal process are redistributed according to the dispersal kernel. Let $N_t(x)$ be the population density at generation t at location x , $S_t(x)$ be the seeds produced at that location, and \hat{S}_t be the seeds redistributed in space after dispersal. We model the distribution of the population of plants at generation $t + 1$ as

$$N_{t+1}(x) = A_t(x) + \beta \hat{S}_t(x). \quad (2.12)$$

where $\hat{S}_t(x)$ is given by

$$\hat{S}_t(x) = \int_{-\infty}^{\infty} K(x, y) S_t(y) dy. \quad (2.13)$$

2.2.3 Dispersal Kernel

The Dispersal kernel describes the spatial probability distribution of the seeds dispersed from a mother plant. It should represent the distribution of seeds generated by the plant's dispersal vector. We address now the modeling of the expansion of a plant dispersed by frugivores birds. Hence, the dispersal kernel for our IDE model should reflect the seed shadow (spatial distribution of seeds) generated by the frugivores birds.

Considering that seeds follow animal movement, we may use the theoretical dispersal kernel derived in chapter 1, through an ecological diffusion and settling model (Powell and Zimmermann, 2004; Neubert et al., 1995; Turchin, 1998),

$$K(x - \xi) = \frac{1}{D(\omega x)} \frac{1}{2\sqrt{\langle D^{-1} \rangle}} \exp^{-|x-\xi|\sqrt{\langle D^{-1} \rangle}}, \quad (2.14)$$

where $D(\omega x)$ is the diffusion function of the animal disperser, or seed in move, and may have the form:

$$D(\omega x) = \left[\frac{1}{2} \sin(\omega x + \frac{\pi}{2}) + \frac{1}{2} \right] + \gamma, \quad (2.15)$$

where γ is the minimum diffusion and ω is the frequency of the settling sites. The constant $\langle D^{-1} \rangle$ represents the harmonic mean of the diffusion function (2.15). The inverse of the diffusion D^{-1} is

known as the residence index, and gives an estimation of the time that the animal stays at a given location (Turchin, 1998; Okubo and Levin, 2001). Hence the parameter γ^{-1} gives an estimation of the time that the disperser spends at a settling site.

The dispersal kernel (2.14) represents the seed dispersal by frugivores animals with periodically settling sites.

2.3 Results

The model is analyzed in three section: i) Local dynamics, ii) Spatial dynamics and iii) Homogenization of the dispersal kernel and average expansion speed.

2.3.1 Local Dynamics: Growth model

The dynamics of the growth model will be analyzed through their equilibria points and stability. For the analyses we use the expression (2.11), which we may write in the general form

$$N_{t+1} = F(N_t) = N_t f(N_t), \quad (2.16)$$

where, $f(N_t)$ is the per capita population growth. From equation (2.16) we have that the equilibria points N^* satisfy, $N^* = 0$ or $f(N^*) = 1$. The trivial point $N_0^* = 0$ always exists. The real roots of $f(N_t) = 1$ yield the non trivial equilibria

$$N_{cr}^* = -\frac{1}{2} \left[(1-q) + \frac{s-rq}{s+1} \right] - \frac{1}{2} \sqrt{\left[(1-q) + \frac{s-rq}{s+1} \right]^2 - \frac{4s(1-q)}{s+1}}, \quad (2.17)$$

$$N_{cr}^* = -\frac{1}{2} \left[(1-q) + \frac{s-rq}{s+1} \right] + \frac{1}{2} \sqrt{\left[(1-q) + \frac{s-rq}{s+1} \right]^2 - \frac{4s(1-q)}{s+1}}, \quad (2.18)$$

The non trivial equilibria depend on the parameters (s, r, q) . The equation $f(N_t) = 1$ is a quadratic polynomial, and applying Descartes rule, we may deduce the existence condition for real roots

$$\frac{s-rq}{s+1} < q-1. \quad (2.19)$$

If condition (2.19) is satisfied, we have 3 equilibria, the trivial equilibrium ($N_0^* = 0$) which is stable, and two nontrivial equilibria, one unstable (N_{cr}^*) and the other stable (N_k^*). The equilibrium point N_{cr}^* , represents a critical density, below this density the population goes extinct, and above it, the population strives and reaches its carrying capacity density, represented by the stable equilibrium

(N_k^*) (Figure 2.2). In this situation we have a strong Allee effect, which establishes critical density in the dynamics of the population growth.

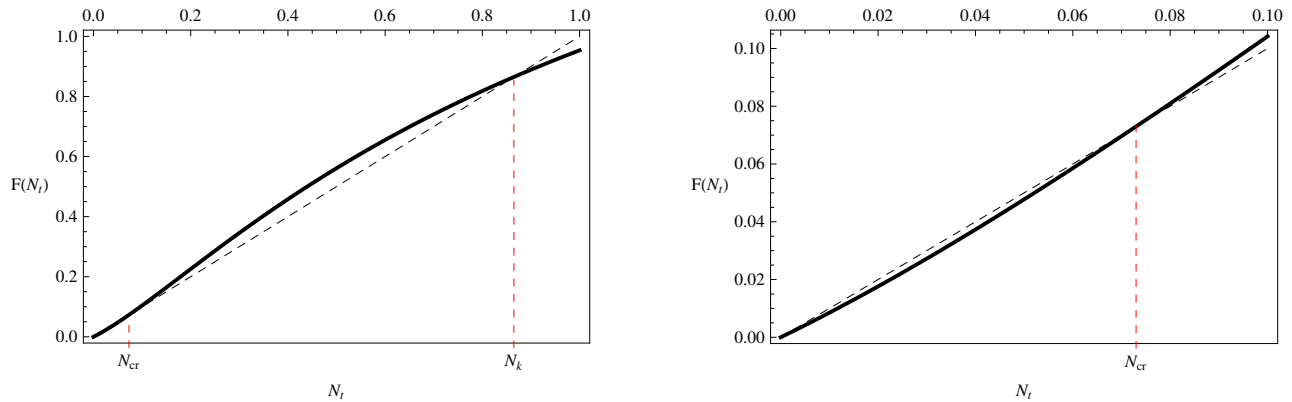


Figure 2.2: Growth Function of a plant subject to an Allee effect. The carrying capacity density N_k and the critical density N_{cr} are shown. To the left is an enlargement of the behavior of the growth function for small densities. It can be observed that for densities $N < N_{cr}$, we have $F(N_t) < 1$ which implies a decline in the population growth. Parameters used: $s = 0,53$; $r = 2,75$; $q = 0,82$.

In Figure 2.3 the bifurcation diagram is shown in relation to the Allee effect for some fixed parameters r and q . It shows the variations of the carrying capacity and critical densities as the Allee effect intensifies.

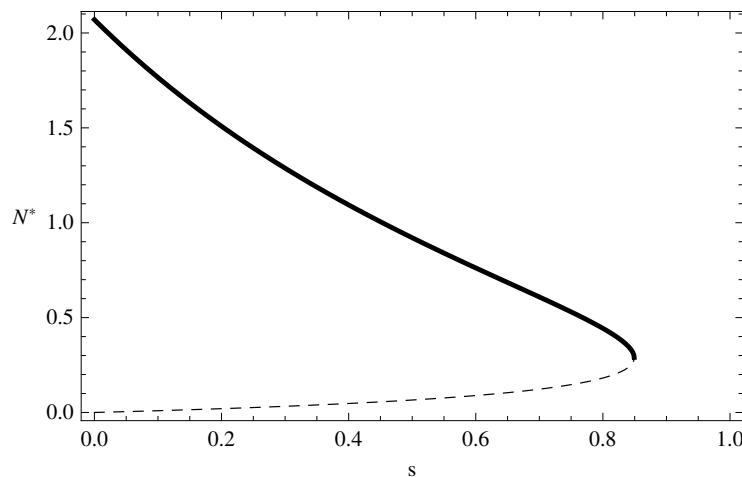


Figure 2.3: Bifurcation diagram for the growth function in relation to the intensity of the Allee effect s . Continuous line: N_k^* ; Dashed line: N_{cr}^* . Parameter values: $r = 2,75$; $q = 0,82$.

2.3.2 Spatial Dynamics: Dispersal Process

First, we analyzed the IDE model for population growth and dispersal (2.12) through numerical simulations. For all the simulations we used the following initial condition

$$N_0(x) = \begin{cases} 0,8 & \text{for } |x| \leq 1, \\ 0 & \text{otherwise.} \end{cases} \quad (2.20)$$

The simulations allowed us to observe the expansion behavior of the plant, through the spatial distribution of the population at any generation time and through the spatial displacement of the invasion front. To find the location of the invasion front at any generation time, we chose a fixed population density N_f , and determine the furthest point from origin at which the population exceeded the preset density. The difference between the front locations of two successive generations, t and $t + 1$, is the spatial displacement of the population.

Population Expansion and Allee effect

Starting with an initial population of (2.20), and for some fixed parameters, the IDE model solution evolves into a propagating and oscillating wave. The population density increases and expands in both directions symmetrically (Figure 2.4.a.). The front wave does not behave as a constant front as a travelling wave, nor as a travelling periodic wave (TPW)(Figure 2.4.b). The shape of the wave front changes from generation to generation, and we did not find any two superimposable waves for any period.

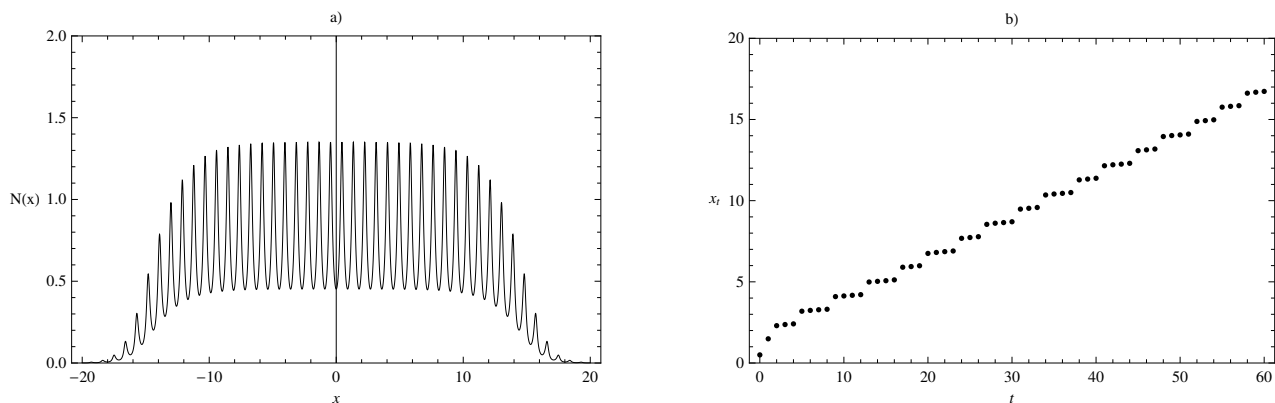


Figure 2.4: a) Spatial population density distribution after 60 generations. b) Population front displacement (x_t) over time (t) (60 generations). Parameter values: i) Growth model: $r = 2,75$; $q = 0,82$; $s = 0,53$. b) Dispersal Kernel: $\omega = 7$; $\gamma = 0,3$.

An interesting feature is the population front displacement. Figure 2.4.b. shows the location of the population front at each generation for some prescribed parameters. It can be observed that

the population front does not advance at a constant rate from generation to generation, instead, the front jumps an approximately constant distance at every 3 to 4 generations, for the group of parameters used for simulation (Figure 2.4.b.). In other words, the population front stagnates at a location, while increasing in density. At the same time seeds are dispersed forward, in larger quantities to the animals' settling sites. These sites may be seen as the potential colonization sites. The population front advances as soon as the next colonization site reaches the preset density N_f . Note that at the wave front, the population is unperceptive ($N < N_f$) in between two successive locations of the population front (x_t and x_{t+3}) (Figure 2.5.). The population emerges first as an isolated populations at the potential colonization sites (or birds settling sites), and then the population islands coalesce with the parent population after some generations, filling the space in between the colonization sites.

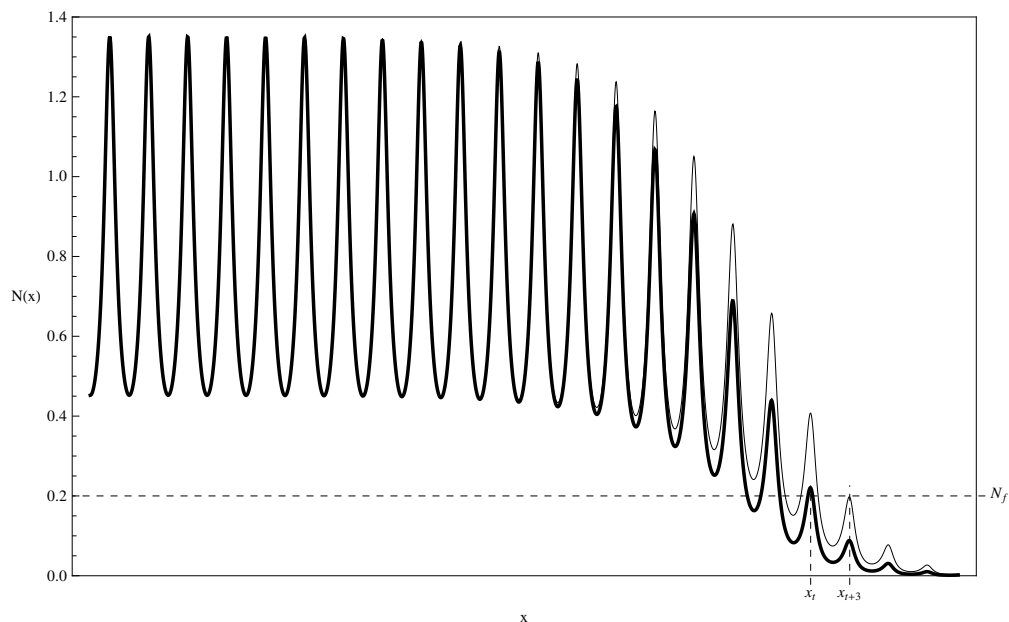


Figure 2.5: Population front displacement. Bold line represents the spatial distribution of the population after 62 generations, and the simple line represents the population distribution after 65 generations. The population front N_f chosen is 0, 2 (horizontal dashed line). The front is located at (x_t) after 62 generations, and at x_{t+3} three generations later ($t = 65$). Parameter values: i) Growth model: $r = 2,75; q = 0,82; s = 0,53$.; ii) Dispersal Kernel: $\omega = 7; \gamma = 0,3$.

The population front stagnation can be seen as the lag phase, in which the population being unperceptive is increasing slowly until it pops up at a new location and then increases rapidly in density. Figure 2.6. shows the population growth at a specific and fixed location. Initially, the population increases slowly followed by a rapid growth, until it stabilizes. In the literature revised, spatially implicit deterministic models have not reported the lag phase behavior observed in our model.

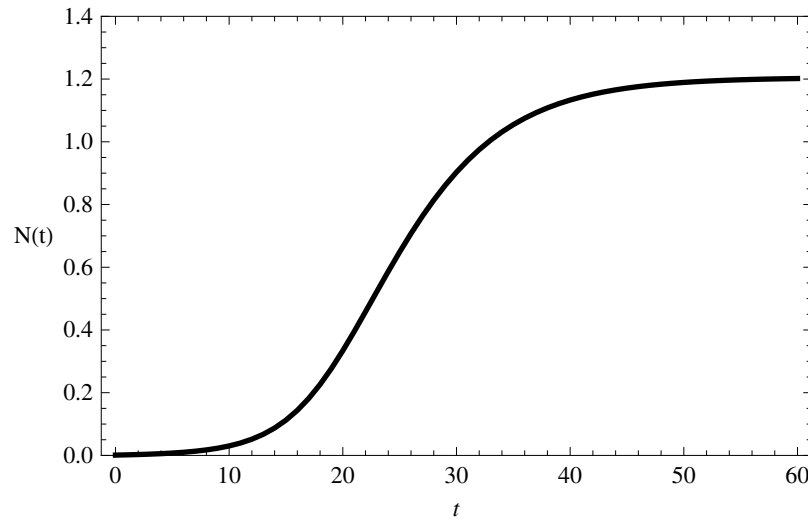


Figure 2.6: Population growth after 60 generations at a fixed location 10.5 distance units from origin. Parameter values: i) Growth model: $r = 2,75; q = 0,82; s = 0,53.$; ii) Dispersal Kernel: $\omega = 7; \gamma = 0,3.$

The intensity of the Allee effect determines the stagnation time of the front or the duration of the lag phase. Figure 2.7 shows the front displacement for different intensities of Allee effect. It is observed that without an Allee effect the front advances at a constant rate. For a subtle Allee effect, the front advances almost at a constant rate, but with increasing intensity the lag phase time of the population front grows, and the front advances at jumps.

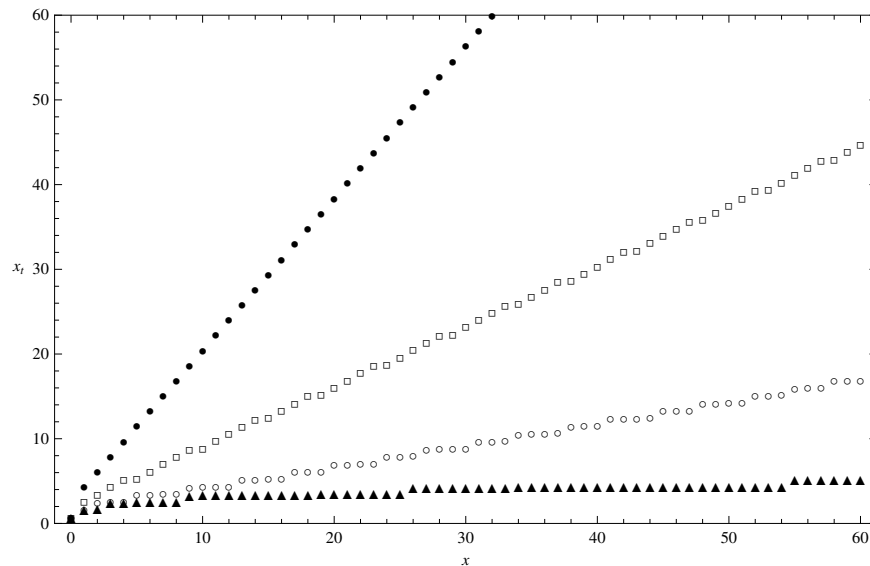


Figure 2.7: Population front for different intensities of the Allee effect (parameter s). a) Black Points: no Allee effect; b) Empty squares: $s = 0,15$; c) Open circles: $s = 0,53$; d) Filled triangles: $s = 0,68$. Parameter values: i) Growth model: $r = 2,75; q = 0,82.$; ii) Dispersal Kernel: $\omega = 7; \gamma = 0,3.$

Population expansion, residence time of dispersers and frequency of settling sites

In chapter 1 we concluded that for smaller values of residence time (γ^{-1}), the tail of the kernel becomes fatter. This means that a seed has a greater chance to travel further distances. We might expect then, that for smaller values of residence time, the population advances faster. Figure 2.8 shows the spatial population distribution after 60 generations for two different values of residence time and holding the other parameters fixed. In fact for a smaller residence time the population expands faster. Figure 2.9.a. shows the front displacement for both values of residence time, and 2.9.b. the magnitude of the step advance of the front. The step advance for the two values of the residence time is very similar, but the lag phase is slightly greater for the expansion with a higher residence time. The difference in the lag phase, makes the population advance faster for a smaller residence time.

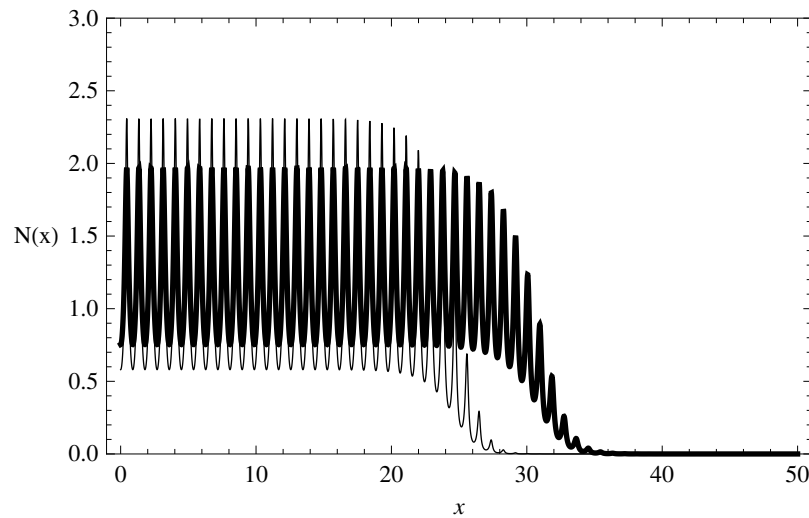


Figure 2.8: Population expansion after 60 generations for two different values of residence time index (γ^{-1}): Bold line: $\gamma^{-1} = 5$; Simple line: $\gamma^{-1} = 2,5$. Parameters' values: i) Growth model: $r = 2,75$; $q = 0,82$; $s = 0,53$; ii) Dispersal Kernel: $\omega = 7$.

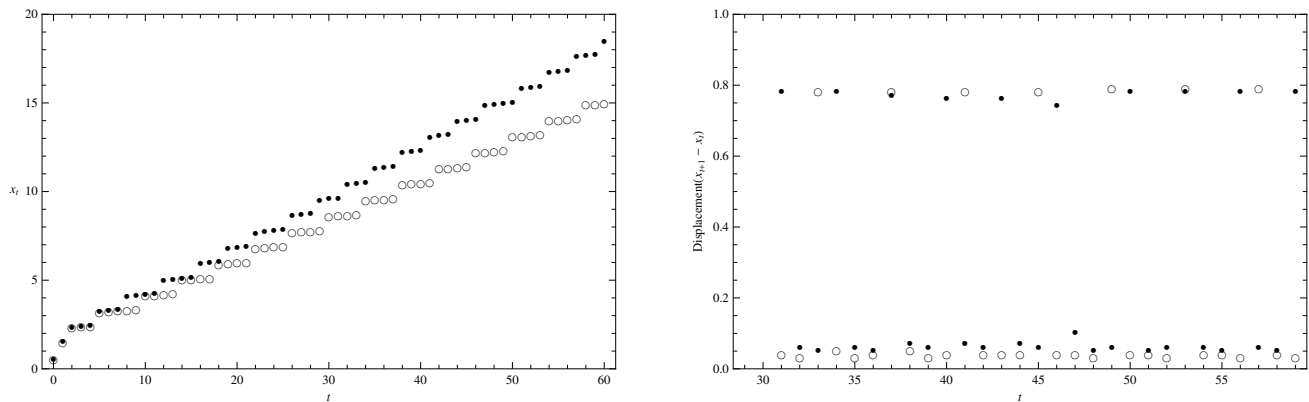


Figure 2.9: Front population location (x_t) in relation to time, for two different values of residence time index (γ^{-1}). Open circles: $\gamma^{-1} = 5$; Filled circles: $\gamma^{-1} = 2, 5$. Parameters' values: i) Growth model: $r = 2, 75$; $q = 0, 82$; $s = 0, 53$; ii) Dispersal Kernel: $\omega = 7$.

In relation to the distance between settling sites, the rate of population expansion was very similar for different distances (Figure 2.10.).

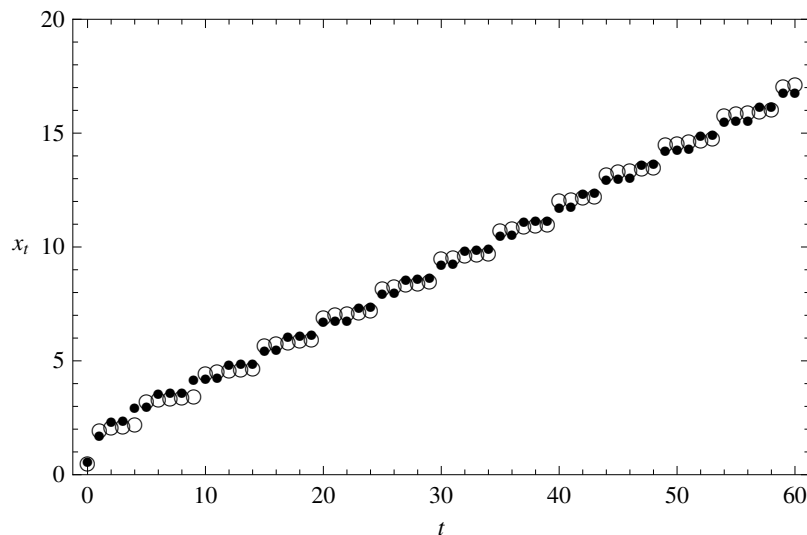


Figure 2.10: Front population location (x_t) in relation to time, for two different frequencies of settling sites. Open circles: $\omega^{-1} = 5$; Filled circles: $\omega^{-1} = 10$. Parameters' values: i) Growth model: $r = 2, 75$; $q = 0, 82$; $s = 0, 53$; ii) Dispersal Kernel: $\gamma = 0, 3$.

Nonetheless, the way the population advances did differ. For shorter distances between settling sites, the population has shorter lag phases, and advances with smaller jumps (Figure 2.11.b. and c.) Conversely for larger distances the lag phase is longer, but the displacement jumps are also bigger (Figure 2.11.a. and c.). As a result, the population advances at a similar rate for every

settling site distance, but with a different expansion behavior. For shorter distances, the behavior of the population expansion resembles more the expansion in homogeneous environments.

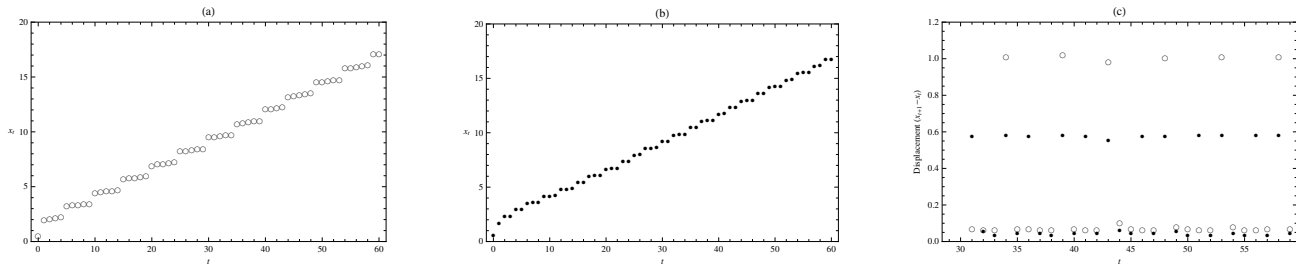


Figure 2.11: Front population location (x_t) in relation to time for two different distances of settling sites ($\frac{2\pi}{\omega}$): a) $\omega_1 = 5$; b) $\omega_2 = 10$. c) Displacement of the front population at every generation time for the two settling site distances : Open circles represent $\omega_1 = 5$ and filled circles $\omega_2 = 10$. Parameter values: i) Growth model: $r = 2,75$; $q = 0,82$; $s = 0,53$.; ii) Dispersal Kernel: $\gamma = 0,3$.

Population expansion speed through an averaged dispersal kernel

In the preceding section we gave an analytical approximation to the step advance of the population expansion. Nonetheless, the step advance does not tell us how fast the population is expanding, unless we know the lag phase period. If we know the duration of the lag phase, we would be able to obtain an averaged expansion speed of the population, dividing the step advance through the lag phase period. From other works (Kot et al., 1996; Wang et al., 2002), we know that for homogeneous environments using homogeneous (not oscillating) dispersal kernels, populations subject to an Allee effect have a continuous expansion with a constant speed through space. This is not our case, but if we could justify and represent our original oscillating dispersal kernel with an averaged and homogeneous kernel, we could give an averaged expansion speed of the population.

The dispersal kernel used for our population expansion model, represents the seed shadow generated by frugivores birds. The spatial patterns in seed distribution generated by frugivores birds, occur at a smaller scale (p.e. habitats within a community) in relation to the scale where plant population expansion takes place (p.e. landscape or regional scale) (Kollmann, 2000). From a macroscale perspective, plant population expansion may be perceived as a continuous wave (advance), where the heterogeneity has been blurred because of the scale, but its effect still remains in the resulting expansion speed.

The oscillations in our dispersal kernel reflect the heterogeneity of the environment, more specifically represent the motility of the animal dispersers through the environment (see chapter 1). This heterogeneity occurs at a smaller scale than plant population expansion. Our objective is to average the heterogeneity of the dispersal kernel in order to obtain a homogeneous kernel, which retains the mean effect of the heterogeneous environment. The dispersal kernel used for modeling population expansion has the expression

$$K(x, y) = \frac{1}{D(x)} \frac{1}{2\sqrt{\langle D^{-1} \rangle}} \exp^{-|x-y|\sqrt{\langle D^{-1} \rangle}}. \quad (2.21)$$

The term $D^{-1}(x)$ is responsible for the oscillating behavior of the kernel, and represents the heterogeneity of the environment. We homogenized the dispersal kernel through averaging the oscillating term as follows

$$\langle D^{-1} \rangle = \frac{1}{p} \int_0^p \frac{1}{D(x)} dx, \quad (2.22)$$

where p is the period of the function $D^{-1}(x)$. Thus the homogenized dispersal kernel is given by

$$K_{hom}(x, y) = \frac{1}{2} \sqrt{\langle D^{-1} \rangle} \exp^{-|x-y|\sqrt{\langle D^{-1} \rangle}}. \quad (2.23)$$

Figure 2.12. shows the original and the homogenized kernel. The homogenized kernel, does not have the oscillating behavior, but retains the mean effect of the environmental heterogeneity. We expect to obtain good estimations on the average expansion speed using this kernel.

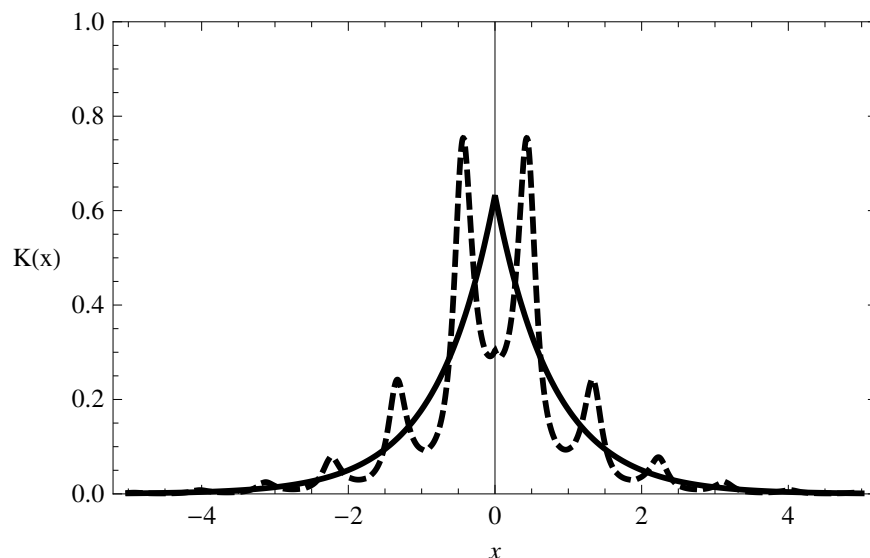


Figure 2.12: Dispersal Kernels: Homogenized dispersal kernel (continuous line); Original dispersal kernel (dashed line). Parameters' values: $\omega = 7$; $\gamma = 0, 3$.

Table 2.1. compares the averaged expansion speeds with the two kernels (original and homogenized) for some parameters of the dispersal kernel. The average expansion speed is calculated over the last half of the generations simulated:

$$c = \sum_{t = T/2}^T \frac{x_{t+1} - x_t}{T/2},$$

where x_t is the position of the front at generation t , and T is the total generations simulated. It can be observed that the homogenized kernel approximates well the averaged expansion speed of the original kernel.

γ	$\langle D^{-1} \rangle$	c	c_{hom}	Relative error $\frac{c_{hom} - c}{c}$
0,4	1,33631	0,292041	0,302449	0,0356
0,3	1,60128	0,272245	0,276327	0,015
0,2	2,04124	0,220816	0,244694	0,108

Table 2.1: Average expansion (c, c_{hom}) speeds yielded by the original (c) and homogenized kernels (c_{hom}). Parameters values: i) Growth function: $r = 2,75; q = 0,82, s = 0,53$; ii) Dispersal Kernel: $\omega = 7$.

Figure 2.13. shows the front displacement for both dispersal kernels for some fixed parameters. The graph shows how well the homogenized kernel approximates the front displacement. It can be observed the linear displacement of the front when using the homogenized kernel, which represents a constant and continuous advance of the front (without lag phases).

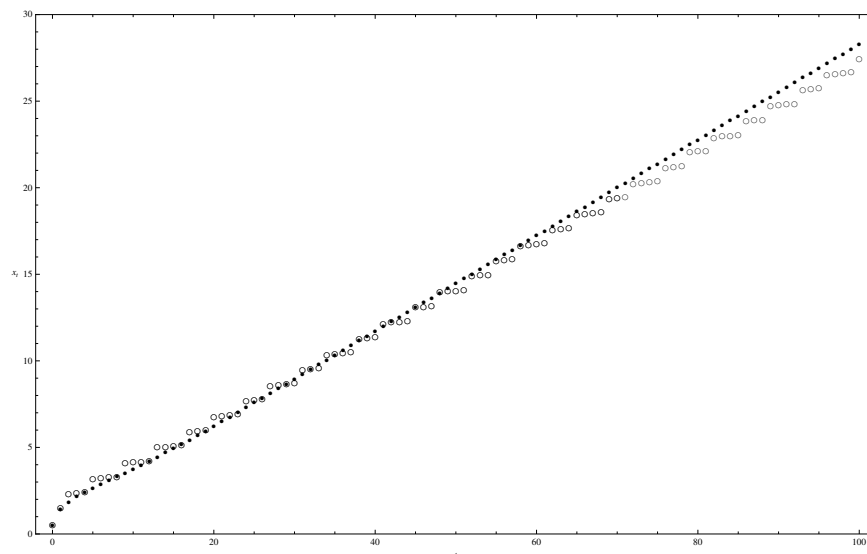


Figure 2.13: Location of the front population (x_t) in relation to time. Open circles: original kernel; Filled circles: homogenized kernel. Parameters' values: i) Growth model: $r = 2,75; q = 0,82; s = 0,53$.; ii) Dispersal Kernel: $\omega = 7; \gamma = 0,3$.

The linear and continuous advance of the front results in a population expanding as a traveling wave. Figure 2.14. compares the population expansion and distribution after 60 generations for the original and homogenized kernel. With the homogenized kernel, the population advances as a travelling wave with a constant front shape. It can be observed that the population behind the front reaches a constant density which corresponds to the carrying capacity N_k .

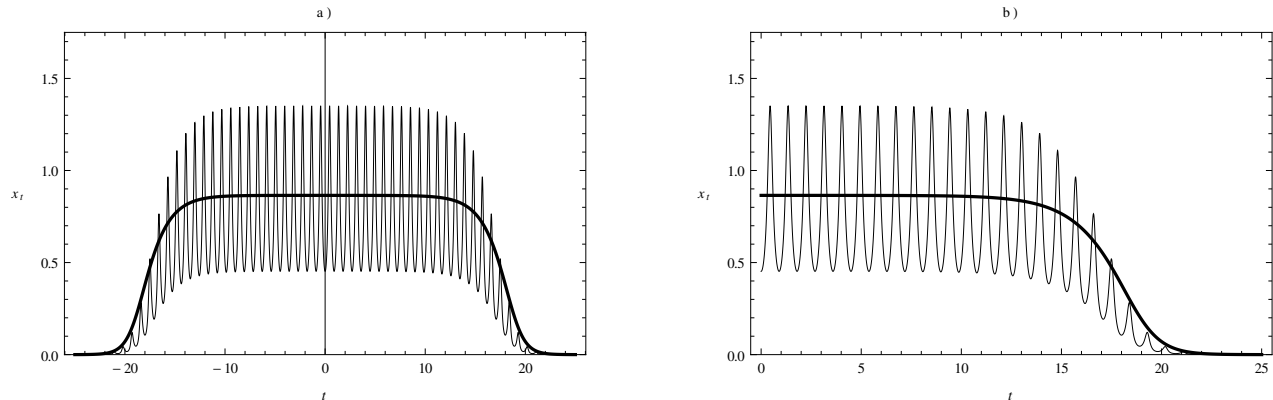


Figure 2.14: a) Population spatial distribution after 60 generations with homogenized kernel (bold line) and original kernel (simple line). b) Front shape of the population expansion. Parameters' values: i) Growth model: $r = 2,75$; $q = 0,82$; $s = 0,53$.; ii) Dispersal Kernel: $\omega = 7$; $\gamma = 0.3$.

2.3.3 Discussion

Population Expansion Behavior

Deterministic models for the dispersal of organisms predict, in general, expansions as traveling waves for homogeneous environments and periodic traveling waves for heterogeneous, yet periodic, environments. Dispersal of organisms using IDE in heterogeneous environments, are beginning to appear. The IDE model here proposed, predicts an expansion of the population as a symmetric propagating wave, without a constant front shape. Kawasaki and Shigesada (2007) also documented a propagating wave without a constant front shape for an IDE in heterogeneous and periodic environment.

An interesting feature in the behavior of the population expansion, is the advance of the invasion front. Our IDE- model does not predict a constant advance of the front, as the majority of deterministic models do (Reaction Diffusion or IDE models), instead our IDE- model predicts a pulsed invasion. A pulsed invasion is defined as a *"regularly punctuated range expansion interspersed among periods of range stasis"* (Johnson et al., 2006). The spread of an organism is often not continuous, but proceeds as discontinuous steps or jumps, forming isolated populations ahead, at

the front of the invasion. These isolated populations, eventually coalesce with the parent population behind, as the space in between is occupied by the expanding population (Liebhold and Tobin, 2008). This expansion behavior is said to be due to a stratified diffusion (Shigesada et al., 1995) or to the combination of stratified diffusion and Allee effect (Johnson et al., 2006). Stratified diffusion is referred as the combination of local and long distance dispersal (Shigesada et al., 1995). From our model, we argue that the pulsed invasion behavior is due to the heterogeneous distribution of seeds dispersed due to the heterogeneity of the environment together with the Allee effect. Dispersal models which involve either environmental heterogeneity or Allee effect alone, have not been able to reproduce the pulsed invasion dynamics. Our results suggests that for small intensities of Allee effect, the expansion proceeds at a roughly constant pace, but for stronger Allee effect a pulsed invasion behavior appears. The term long distance dispersal is relative, and in accordance with Shigesada et al. (1995), we may consider a long distance dispersal, the dispersal of seeds at the periphery of the range, producing nascent colonies ahead of the parent range, which will merge after a few generations. These type of stratified diffusion produces a biphasic expansion, an initially slow advance followed by a greater and linear expansion rate (Shigesada et al., 1995). Our model captures just the second phase of the linear expansion rate.

The Allee effect has been responsible for the lag phases observed in biological invasions. The lag phase is the period of time that it takes for an invader to reach considerable numbers to be noticed locally, and to be able to spread. The dynamics of our model, shows that, the Allee effect, indeed, may be responsible for certain lag phases observed in some biological invasions. Traditional dispersal models with Allee effect, have put in evidence the reduction in the expansion speed, but have failed to show the lag phase. The front stagnation and the sudden jump of the front may be an evidence of the lag phases at the front of the invasion. Through our model, it can be seen that, during the front stasis at a certain location, the population is dispersing its seeds forward, in larger amounts to those sites the animal dispersers use to settle. These settling sites may be seen as the new localities of colonization. Here, the population begins to increase slowly, until it reaches certain density levels and grows rapidly and pops up as a new colonization site, at the periphery of the parent population range. The stronger the intensity of the Allee effect, the longer the stagnation period and the lag phase.

Expansion Speed, Landscape Structure and Birds Motility

The landscape structure is introduced in the model through the frequency or distance between settling site. The settling sites are habitats within a community or vegetation features in the habitats, which the frugivores birds use to settle for longer periods of time. Our results suggest that the distance between settling sites do not affect the expansion speed of the population. For different distance between settling sites the expansion speed is very similar. Nonetheless, the behavior of the front displacement did change. For larger distances, the population shows longer lag phase, and the magnitude of the jump displacement is higher. Conversely, for smaller distances the step of advance and the lag phase are smaller. As the settling sites become nearer from each

other, the population advances in a more continuous and constant pace. For settling sites more apart from each other, the impulsive invasion behavior is more evident. We may conclude that the landscape structure may not influence the expansion speed, but it determines the behavior of the expansion, if it is a roughly continuous or impulsive invasion.

On the other hand, the bird's motility, has an effect on the expansion speed, since it modifies the tail of the dispersal kernel (see chapter 1). For smaller residence time at the settling sites, the dispersal kernel has a fatter tail, which increases expansion speeds (Kot et al., 1996). Conversely, for larger residence time, we have a thinner tail, yielding a lower expansion speed. Our results are in agreement with the above statements, having higher expansion speeds for smaller residence time at the settling sites.

Average Dispersal Kernel and Expansion Speed

Our results show a pulsed invasion behavior for the population expansion. This expansion dynamics is attributable to heterogeneous environment influencing the motility of the animals seed dispersers and the Allee effect. The heterogeneity introduced in the model occurs at a smaller scale than that of population expansion, hence this may justify a homogenization of the dispersal kernel. For the purpose of calculating expansion speeds, the homogenization of the dispersal kernel proved to be successful in estimating the averaged expansion speed. Although, the homogenized kernel models population expansion, as if it is spreading in a homogeneous environment, its parameters have the mean effect of the heterogeneous environment. Homogenization techniques which average the effect of heterogeneous media have been useful in modeling the diffusion of substances or the spreading of organisms (Holmes, 1995; Dewhurst and Lutscher, 2009, Powell and Zimmermann, 2004; Garlick et al., 2011).

2.4 Conclusions

In general, IDE or RDE (reaction diffusion equations) models for the dispersal of organisms, predict a continuous and constant (or accelerated sometimes) advance of the population front. Our IDE model for the dispersal of a plant in a heterogeneous environment and subject to Allee effect, contrary to a continuous invasion, predicted a pulsed invasion behavior. As far as we know, these behavior has not been reproduced by a IDE or RDE model.

The pulsed invasion is accentuated as the intensity of the Allee effect increases. For subtle intensities of the Allee effect, the population advances at a roughly constant rate. We may conclude that the pulsed invasion behavior is due to heterogeneity of the environment, and principally to the Allee effect, as has been suggested by other authors as is the case of the gypsy moth (Johnson et al., 2006)).

Our model, also may support the hunch that the Allee effect may be responsible for the lag phase in the invasion process (Parker, 2004; Taylor and Hastings, 2005). During the front stagnation, seeds are dispersing ahead of the population, contributing to the formation of new colonies. Initially, these new colonies may grow very slowly, due to the Allee effect, until they reach a density level where they experience a rapid grow, popping up as an isolated colonies. These colonies will merge after a few generations with the parent population.

Integro-difference model for the dispersal of organisms, use dispersal kernels which assume homogeneous environments. Our expansion speeds estimated with the dispersal kernel for heterogeneous environment were well approximated by the speeds obtained by the homogenized dispersal kernel. We may conclude that for expansion speeds we may take a dispersal kernel for homogeneous environment, but its parameters should contain the mean effects of the heterogeneity.

Conclusões Gerais

Os modelos íntegro- recursivos tem ganhado popularidade para a modelagem de dispersão de organismos com fases bem definidas e separadas de reprodução e dispersão. A popularidade deve-se principalmente, à fácil incorporação de diferentes padrões de dispersão através dos núcleos de dispersão.

A derivação de núcleos de dispersão é um problema atual e de grande relevância pois influencia a velocidade de expansão dos organismos. Para o caso de dispersão de plantas, em que as sementes são a parte da população que se dispersa, tem-se utilizado distribuições que descrevem uma diminuição contínua da densidade de sementes com a distância desde a fonte (planta mãe). Este comportamento pode não se aplica para plantas que se dispersam por animais, onde tem-se observado uma distribuição de agregação.

Núcleos de dispersão teóricos para a sementes dispersadas por vento tem sido desenvolvidos satisfatoriamente, porém para sementes dispersadas por animais, não ocorre o mesmo, principalmente pela dificuldade de modelar o comportamento e movimento dos animais. No entanto existem algumas tentativas, que se baseiam nos modelos de difusão e sedimentação. Seguindo este marco teórico de difusão e sedimentação, e usando a " *difusão ecológica* " ao invés da difusão de Fick, para a modelagem do movimento dos animais, conseguiu-se gerar um núcleo de dispersão que reproduz a distribuição agregada das sementes dispersadas por animais. Os sítios de acumulação de sementes representam as localidades onde os animais apresentam menor movimentação no ambiente. Observamos que quanto maior mobilidade apresentam os animais, a cauda da distribuição fica mais grossa, o que repercute em um aumento na velocidade de expansão da população de plantas. Consideramos que os modelos de difusão e sedimentação oferecem um marco teórico simples e adequado para desenvolver núcleos de dispersão por animais.

A técnica de múltiplas escalas e homogeneização foi adequada para aproximar analiticamente o núcleo de dispersão, pois a aproximação reteve a distribuição agregada das sementes.

A modelagem da expansão de uma planta sujeita a efeito Allee e com dispersão por animais apresentou comportamentos não observados antes por modelos tradicionais de reação e difusão e integrodiferenciais. Em geral estes modelos mostram uma expansão da população de forma contínua e constante. Através do modelo aqui proposto, observou-se uma expansão a pulsos " *pulsed invasion* ", caracterizada por um estancamento da frente da invasão por um período de tempo e seguido de um avanço em forma de salto. Este comportamento é devido à combinação da

heterogeneidade do ambiente e o efeito Allee. Este comportamento mais acentuado quanto maior é a intensidade do efeito Allee. Este comportamento de expansão tem sido registrado em invasões de alguns organismos como a invasão da mariposa cigana "*gypsy moth*" nos Estados Unidos, e da formiga argentina "*Linepithema humile*" (Suarez et al., 2000).

Dos resultados, obtidos sobre o comportamento do avanço da população, concluímos, que o efeito Allee pode ser um dos fatores responsáveis do período de latência "*lag phase*" observado em algumas invasões como sugerido por alguns autores (Parker, 2004, Taylor and Hastings, 2005). Durante o período de estancamento da frente, as colônias formando-se na frente da invasão crescem aos poucos aparecerem como ilhas, que posteriormente fundem-se com o resto da população.

Para fins de estimar a velocidade de expansão da população resulta conveniente homogeneizar o núcleo de dispersão, para obter a velocidade média de expansão da população. Se bem o núcleo homogêneo prediz a velocidade de expansão, ele não apresenta o comportamento do avanço da população, isto é a invasão através de pulsos. Concluímos que núcleos resultantes de ambientes homogêneos predizem bem a velocidade de expansão de populações, desde que os parâmetros representem os efeitos médios dos ambientes heterogêneos.

Bibliografia

- D.S. Boukal and L. Berec. Single-species models of the allee effect: Extinctions boundaries, sex ratios and mate encounters. *Journal of Theoretical Biology*, 218:375–394, 2002.
- C. Clark, J.R. Poulsen, B.M. Bolker, E.F. Connor, and V.T. Parker. Comparative seed shadows of bird-, monkey-, and wind-dispersed trees. *Ecology*, 86:2684–2694, 2005.
- H. Davis, C.M. Taylor, J.G. Lambrinos, and D.R. Strong. Pollen limitation causes an Allee effect in a wind-pollinated invasive grass (*Spartina alterniflora*). *PNAS*, 101(38):13804–13807, 2004.
- S. Dewhurst and F. Lutscher. Dispersal in heterogeneous habitats: thresholds, spatial scales, and approximate rates of spread. *Ecology*, 90(5):1338–1345, 2009.
- M.J. Garlick, J.A. Powell, M.B. Hooten, and L.R. MacFarlane. Homogenization of large-scale movement models in ecology. *Bull Math Biol*, 73:2088–2108, 2011.
- C. Gosper, C.D. Stansbury, and G. Vivian-Smith. Seed dispersal of fleshy-fruited invasive plants by birds: contributing factors and management options. *Diversity and Distributions*, 11:549–558, 2005.
- M.J. Groom. Allee effects limit population viability of an annual plant. *The American Naturalist*, 151(6):487–496, 1998.
- A. Hastings, K. Cuddington, K. Davis, C. Dugaw, C. Elmendorf, and S. Freestone. The spatial spread of invasions. *Ecology Letters*, 8:91–101, 2005.
- M.H. Holmes. *Introduction to Perturbation Methods*. Springer-Verlag, New York, 1995.
- D.M. Johnson, A.M. Liebhold, P.C. Tobin, and O. Bjornstad. Allee effects and pulsed invasion by the gypsy moth. *Nature*, 444(16):361–363, 2006.
- K. Kawasaki and N. Shigesada. An integrodifference model for biological invasions in a periodically fragmented environment. *Japan Journal of Industrial and Applied Mathematics*, 24:3–15, 2007.
- J. Kollmann. Dispersal of fleshy-fruited species: a matter of spatial scale? *Perspectives in Plant Ecology, Evolution and Systematics*, 3(1):29–51, 2000.

- M. Kot. Discrete-time travelling waves: Ecological examples. *Journal of Mathematical Biology*, 30:413–436, 1992.
- M. Kot, M. Lewis, and P. van den Driessche. Dispersal data and the spread of invading organisms. *Ecology*, 77(7):2027–2042, 1996.
- S. Levin, H.C Muller-Landau, R. Nathan, and J Chave. The Ecology and Evolution of Seed Dispersal: A Theoretical Perspective. *Annual Review Ecology, Evolution and Systematics*, 34: 575–604, 2003.
- M.A. Lewis and P. Kareiva. Allee dynamics and the spread of invading organisms. *Theoretical Population Biology*, 43:141–158, 1993.
- A.M. Liebhold and P.C. Tobin. Population ecology of insect invasion and their management. *Annual Review of Entomology*, 53:387–408, 2008.
- D.C. Mistro, L.A. Diaz Rodrigues, and S. Petrovskii. Spatiotemporal complexity of biological invasion in a space and time discrete predator prey system with the strong Allee effect. *Ecological Complexity*, 9:16–32, 2012.
- D.A. Murray. Avian seed dispersal of three neotropical gap-dependent plants. *Ecological Monographs*, 58(4):271–298, 1988.
- R. Nathan and H.C. Muller-Landau. Spatial Patterns of Seed Dispersal, their Determinants and Consequences for Recruitment. *Trends in Ecology and Evolution*, 15(7):278–285, 2000.
- M. Neubert, M. Kot, and M.A. Lewis. Dispersal and Pattern Formation in a Discrete-Time Predator-Prey Model. *Theoretical Population Biology*, (48):7–43, 1995.
- A. Okubo and S. Levin. A Theoretical Framework for Data Analysis of Wind Dispersal of Seeds and Pollen. *Ecology*, 70(2):329–338, 1989.
- A. Okubo and S.A. Levin. *Diffusion and Ecological Problems*. Springer Verlag, New York, 2001.
- I. Parker. Mating patterns and rates of biological invasion. *PNAS*, 101(38):13695–13696, 2004.
- S. Petrovskii, A. Morozov, and E. Venturino. Allee effect makes possible patchy invasion in a predator-prey system. *Ecology Letters*, 5:345–352, 2002.
- J. Powell and N.E. Zimmermann. Multi-scale analysis of active seed dispersal contributes to resolving reid’s paradox. *Ecology*, 85(2):490–506, 2004.
- S.E. Russo, S. Portnoy, and C.K. Auspurger. Incorporating Animal Behavior into Dispersal Models: Implications for Seed Shadows. *Ecology*, 87(12):3160–3174, 2006.
- N. Shigesada, K. Kawasaki, and Y. Takeda. Modeling stratified diffusion in biological invasions. *The American Naturalist*, 146(2):229–251, 1995.

- P.A. Stephens, W.J. Sutherland, and R.P. Freckelton. What is the Allee effect? *Oikos*, 87(1): 185–190, 1999.
- A.V. Suarez, D.A. Holway, and T.T. Case. Patterns of spread in biological invasions dominated by long-distance jump dispersal: insights from argentine ants. *PNAS*, 98:1095–1100, 2000.
- F. Takasu, N. Kawasaki, K. Togashi, K. Kishi, and N. Shigesada. Modeling the expansion of an introduced tree disease. *Biological Invasions*, 2:141–150, 2000.
- C.M. Taylor and A. Hastings. Allee effect in biological invasions. *Oikos*, 8:895–908, 2005.
- P. Turchin. *Quantitative Analysis of Movement*. Sinauer Associates, Inc. Publishers, Sunderland, Massachusetts, 1998.
- M. Wang, M. Kot, and M. Neubert. Integrodifference equations, allee effect and invasions. *Journal of Mathematical Biology*, 44:150–168, 2002.
- D.A. Westcott, J. Bentrupperbaumer, M.G. Bradford, and A. McKeown. Incorporating patterns of disperser behavior into models of seed dispersal and its effects on estimated dispersal curves. *Oecologia*, (146):57–67, 2005.